

Efficient Bayesian inference for univariate and multivariate non linear state space models with univariate autoregressive state equation

Alexander Kreuzer * Claudia Czado

Zentrum Mathematik, Technische Universität München

July 19, 2022

Abstract

Latent autoregressive processes are a popular choice to model time varying parameters. These models can be formulated as non linear state space models for which inference is not straightforward due to the high number of parameters. Therefore maximum likelihood methods are often infeasible and researchers rely on alternative techniques, such as Gibbs sampling. But conventional Gibbs samplers are often tailored to specific situations and suffer from high autocorrelation among repeated draws. We present a Gibbs sampler for general non linear state space models with an univariate autoregressive state equation. We employ an interweaving strategy and elliptical slice sampling to exploit the dependence implied by the autoregressive process. The sampler shows good performance for established models, such as stochastic volatility models with Gaussian and skew Student t errors as well as for dynamic bivariate copula models. Additionally, we use the sampler to estimate the parameters of a proposed bivariate dynamic mixture copula model. This model allows for dynamic asymmetric tail dependence and is employed to model the volatility return relationship. Comparison to relevant benchmark models, such as the DCC-GARCH or a Student t copula model, with respect to log predictive likelihoods shows the superior performance of the proposed approach.

1 Introduction

There are many situations where statistical models with constant parameters are no longer sufficient to appropriately represent certain aspects of the economy. For example it is well known that volatility of financial assets changes over time (Schwert (1989)). This is why many models that allow for variation in the parameter have been proposed. There are time varying vector autoregressive models (Primiceri (2005), Nakajima et al (2011)), stochastic volatility models (Kim et al (1998)), GAM copula models (Vatter and Chavez-Demoulin (2015), Vatter and Nagler (2018)) and many more. Stochastic volatility models and the bivariate dynamic copula model of Almeida and Czado (2012) assume that the parameter follows a latent autoregressive process of order 1 (AR(1) process). These two models belong to the class of models that we will study.

In a time varying parameter framework we consider a d dimensional random variable at time t , $\mathbf{Y}_t \in \mathbb{R}^d$, which is generated from a d dimensional density $f(\cdot|h_t)$. We are interested in models, where the density $f(\cdot|h_t)$ has a univariate dynamic parameter h_t following an AR(1) process. These models can be formulated as state space models with observation equation

$$\mathbf{Y}_t \sim f(\mathbf{y}_t|h_t) \text{ independently,} \quad (1)$$

for $t = 1, \dots, T$. The state equation describes an AR(1) process with mean parameter $\mu \in \mathbb{R}$, persistence parameter $\phi \in (-1, 1)$ and standard deviation parameter $\sigma \in (0, \infty)$ and is given by

$$h_t = \mu + \phi(h_{t-1} - \mu) + \sigma\epsilon_t, \quad (2)$$

*Corresponding author: E-mail: a.kreuzer@tum.de

where $\epsilon_t \sim N(0, 1)$ iid for $t = 1, \dots, T$ and $h_0 \sim N\left(\mu, \frac{\sigma^2}{1-\phi^2}\right)$. In the state equation we assume Gaussian innovations ϵ_t but in the observation equation we do not put restrictions on the density f . Thus we allow for non linear and non Gaussian state space models. Several established models can be analysed within this framework.

By choosing $f(\cdot|h_t)$ as the normal density with mean 0 and variance $\exp(h_t)$, denoted by $\varphi(\cdot|0, \exp(h_t))$, we obtain the stochastic volatility model (Kim et al (1998)) given by

$$\begin{aligned} Y_t &\sim \varphi(y_t|0, \exp(h_t)) \text{ independently,} \\ h_t &= \mu + \phi(h_{t-1} - \mu) + \sigma\epsilon_t, \end{aligned} \tag{3}$$

for $t = 1, \dots, T$. By describing the log variance with a latent AR(1) process this model allows for time varying volatility. Time varying volatility is a stylized fact of financial time series. In this context, the stochastic volatility model has also shown better performance than the frequently used GARCH models (Engle (1982), Bollerslev (1986)) for several data sets (Yu (2002), Chan and Grant (2016)). To allow for heavy tails and skewness, other distributions have been considered in the observation equation. One example is the stochastic volatility model with skew Student t errors (Abanto-Valle et al (2015)), which can also be analysed within our framework.

Dependence modeling is another research area, where models that allow for time varying parameters have been introduced. Vine copulas (Bedford and Cooke (2001), Aas et al (2009)) are widely used models to capture complex dependence structures. To name a few, Brechmann and Czado (2013) and Nagler et al (2018) employ vine copulas for forecasting the value at risk of a portfolio, Aas (2016) gives an overview of applications of vine copulas in finance including asset pricing, credit risk management and portfolio optimization and ? model the association pattern between gap times with D-vine copulas to study asthma attacks. A vine copula model is made up of different bivariate copulas with corresponding dependence parameters. Since dependencies may change over time, extensions that allow for variation in the dependence parameter have been proposed. Vatter and Chavez-Demoulin (2015) introduce a bivariate copula model, where the dependence parameter follows a generalized additive model. Another approach is the dynamic bivariate copula model proposed by Almeida and Czado (2012) and Hafner and Manner (2012), which we will analyse within our state space framework. For this model, we consider one parametric copula families for which there is a one to one correspondence between the copula parameter, denoted by θ , and Kendall's τ . So we can express Kendall's τ as a function of the copula parameter θ and we write $\tau(\theta)$. The restriction of Kendall's τ to the interval (-1,1) is removed by applying the Fisher' Z transformation $F_Z(x) = \frac{1}{2} \log\left(\frac{1+x}{1-x}\right)$. This transformed time varying Kendall's τ is then modeled by an AR(1) process. More precisely, we consider T bivariate random vectors, $(U_{t1}, U_{t2})_{t=1, \dots, T} \in [0, 1]^{T \times 2}$, corresponding to T time points. We assume for $t = 1, \dots, T$ that

$$\begin{aligned} (U_{t1}, U_{t2}) &\sim c(u_{t1}, u_{t2}; \theta_t) \text{ independently} \\ h_t &= \mu + \phi(h_{t-1} - \mu) + \sigma\epsilon_t, \end{aligned} \tag{4}$$

where $h_t = F_Z(\tau(\theta_t))$ and $c(u_{t1}, u_{t2}; \theta_t)$ is a bivariate copula density with parameter θ_t .

Non linear state space models as specified with (1) and (2) are typically difficult to estimate, since there is a large number of parameters and likelihood evaluation requires high dimensional integration. This often makes maximum likelihood approaches infeasible. Gibbs sampling (Geman and Geman (1984)) is a frequently used Bayesian approach to infer parameters of such non linear state space models (Carlin et al (1992)). But the posterior samples, resulting from conventional Gibbs sampling, often suffer from high autocorrelation. Furthermore, the availability of the full conditional distributions or at least an efficient MCMC approach to sample from them is required. This is often tailored to specific situations. We present a Gibbs sampling approach that is designed to handle models with a latent AR(1) process and general likelihood functions as specified by the state space formulation in Equations (1) and (2). To sample from the associated posterior distribution we rely on elliptical slice sampling (Murray et al (2010)) and on an ancillarity sufficiency interweaving strategy (Yu and Meng (2011)). Elliptical slice sampling is used to sample the latent states. This allows us to exploit the Gaussian dependence structure, that is implied by the AR(1) process. But even if we provide efficient methods to

sample from the full conditionals, the sampler may still suffer from the dependence among the repeated draws of the parameters. Additionally, its performance may vary for different model parameterizations (Frühwirth-Schnatter and Sögner (2003), Strickland et al (2008)). This problem is tackled with the ancillarity sufficiency interweaving strategy, where the parameters of the latent AR(1) process are sampled from two different parameterizations. The decision between two parameterizations is avoided by using both. This approach has already shown good results for several models, including univariate and multivariate stochastic volatility models (Kastner and Frühwirth-Schnatter (2014), Kastner et al (2017)).

Further, we propose a dynamic copula model allowing for asymmetric tail dependence in which inference is straightforward with the proposed sampler. The model is a dynamic mixture of a Gumbel and a Student t copula and can be seen as an alternative to the symmetrized Joe-Clayton copula of Patton (2006). The necessity of such models, that allow for dynamic asymmetric tail dependence, was already observed by Patton (2006) for exchange rates data. It will here be illustrated with an application to different financial data. In particular, we study the volatility return relationship, i.e. the dependence between an index and the corresponding volatility index. It is important to provide appropriate models for this relationship, since it has influence on hedging and risk management decisions (Allen et al (2012)). More precisely, we investigate the American index S&P500 and its volatility index the VIX as well as the German index DAX and the VDAX.

For our analysis we make use of a two step approach commonly used in copula modeling (Joe and Xu (1996)) motivated by Sklar’s Theorem (Sklar (1959)). We first model the marginal distribution with a univariate skew Student t stochastic volatility model. In the second step we estimate the dependence among the marginals with the dynamic mixture copula model allowing for time varying asymmetric tail dependence. This flexible model is able to capture several characteristics of the joint distribution of volatility and return. With respect to the marginal distribution we observe positive skewness for volatility indices compared to slight negative skewness for the return indices. In the dependence structure we observe asymmetry and time variation. Finally, we compare the proposed model to several restricted models with constant or symmetric dependence and to a bivariate DCC-GARCH model (Engle (2002)). Model comparison with respect to log predictive likelihoods shows the superiority of our approach.

To summarize, the contributions of this paper are as follows: First we provide an approach to efficiently sample from the posterior distribution of general non linear state space models as specified by Equations (1) and (2). In addition to that, we propose a dynamic mixture copula for time varying asymmetric tail dependence. We discuss Bayesian inference for this model class and demonstrate how it can be utilized to model the volatility return relationship.

2 Bayesian inference

In the following, we denote an observation of the d -dimensional random vector \mathbf{Y}_t by \mathbf{y}_t and the associated data matrix is given by $Y = (\mathbf{y}_1, \dots, \mathbf{y}_T)^t \in \mathbb{R}^{T \times d}$. To subset vectors and matrices we make use of the following notation: For sets of indices A and B we set $\mathbf{x}_A = (x_i)_{i \in A}$ for a vector \mathbf{x} and $X_{A;B} = (x_{ij})_{i \in A, j \in B}$ for a matrix X . We use a capital letter to refer to a matrix and small letters to refer to its components. The set $\{n, \dots, k\}$ of integers will be abbreviated by $n : k$.

We consider the state space model as specified by Equations (1) and (2). To obtain a fully specified Bayesian model we equip the parameters μ , ϕ and σ with prior distributions. We follow Kastner and Frühwirth-Schnatter (2014), who propose the following prior distributions for the latent AR(1) process of the stochastic volatility model:

$$\mu \sim N(0, \sigma_\mu), \quad \frac{\phi + 1}{2} \sim \text{Beta}(a_\phi, b_\phi), \quad \sigma^2 \sim \text{Gamma}\left(\frac{1}{2}, \frac{1}{2B_\sigma}\right), \quad (5)$$

where $\sigma_\mu, a_\phi, b_\phi, B_\sigma > 0$. Our standard choice for the prior hyperparameters is $\sigma_\mu = 100$, $a_\phi = 5$, $b_\phi = 1.5$ and $B_\sigma = 1$ as in Kastner (2016a). With these prior distributions our Bayesian model is complete. For sampling from the posterior distribution of this model we should take into account that sampling efficiency may highly depend on the model parameterization (Frühwirth-Schnatter and Sögner (2003), Strickland et al (2008)). Yu and Meng (2011) differentiate between two parameterizations: A sufficient augmentation and an ancillary augmentation

scheme. In our case a sufficient augmentation is characterized by an observation equation that is free of the parameters μ, ϕ and σ and only depends on the latent states $\mathbf{h}_{1:T}$. In this case $\mathbf{h}_{1:T}$ is a sufficient statistics for the parameters μ, ϕ and σ . In an ancillary augmentation the state equation is independent of the parameters μ, ϕ and σ , then $\mathbf{h}_{1:T}$ is an ancillary statistics for the parameters μ, ϕ and σ . The standard parameterization of our model is already a sufficient augmentation and we refer to this parameterization as given by Equations (1) and (2) as (SA).

$$(SA) : \quad \begin{aligned} \mathbf{Y}_t &\sim f(\mathbf{y}_t | h_t) \text{ independently} \\ h_t &= \mu + \phi(h_{t-1} - \mu) + \sigma \epsilon_t. \end{aligned}$$

An ancillary augmentation is obtained by the following parameterization

$$\tilde{h}_t = \frac{h_t - \mu - \phi(h_{t-1} - \mu)}{\sigma}, \text{ with inverse } h_t = \mu + \phi(h_{t-1} - \mu) + \sigma \tilde{h}_t, \quad (6)$$

for $t = 1, \dots, T$. This reparameterization is obtained by solving Equation (2) for ϵ_t and implies that the state space model is given by

$$(AA) : \quad \begin{aligned} \mathbf{Y}_t &\sim f(\mathbf{y}_t | h_t(\tilde{\mathbf{h}}_{1:T}, h_0, \mu, \phi, \sigma)) \text{ independently} \\ \tilde{h}_t &\sim N(0, 1) \text{ independently,} \end{aligned}$$

where $h_t(\tilde{\mathbf{h}}_{1:T}, h_0, \mu, \phi, \sigma)$ is the function that calculates h_t according to (6). We refer to this model representation as (AA). Instead of deciding between (SA) and (AA), we combine them in an ancillarity sufficiency interweaving strategy (Yu and Meng (2011)), given by

- a) Sample $\mathbf{h}_{0:T}$ in (SA) from $\mathbf{h}_{0:T} | Y, \mu, \phi, \sigma$ (Section 2.1).
- b) Sample (μ, ϕ, σ) in (SA) from $\mu, \phi, \sigma | Y, \mathbf{h}_{0:T}$ (Section 2.2).
- c) Move to (AA) via $\tilde{h}_t = \frac{h_t - \mu - \phi(h_{t-1} - \mu)}{\sigma}$, for $t = 1, \dots, T$.
- d) Sample (μ, ϕ, σ) in (AA) from $\mu, \phi, \sigma | Y, h_0, \tilde{\mathbf{h}}_{1:T}$ (Section 2.3).
- e) Move back to (SA) via the recursion $h_t = \mu + \phi(h_{t-1} - \mu) + \sigma \tilde{h}_t$ for $t = 1, \dots, T$.

Kastner and Frühwirth-Schnatter (2014) employed interweaving for the stochastic volatility model and showed its superior performance with an extensive simulation study. For the stochastic volatility model, Kastner and Frühwirth-Schnatter (2014) propose to move between a sufficient augmentation and a reparameterization of the latent states $\mathbf{h}_{1:T}$ given by $h_t^K = \frac{h_t - \mu}{\sigma}$. Within this reparameterization parameters can be sampled conveniently from its full conditional distribution by recognizing a linear regression model. This is possible for the standard stochastic volatility model, but not in our case since our sampler is designed to handle more general likelihood functions. Therefore we have chosen the reparameterization of (SA) such that it is optimal in the sense of Yu and Meng (2011), i.e. we move between a sufficient and a ancillary augmentation.

Note that reducing the sampler to the first two steps a) and b) results in a standard Gibbs sampler in (SA). This sampler typically suffers from the dependence among the parameters μ, ϕ, σ and the latent states $\mathbf{h}_{1:T}$ in the posterior distribution.

2.1 Sampling of the latent states in the sufficient augmentation

To sample the latent states $\mathbf{h}_{0:T}$ from its full conditional in (SA) we make use of elliptical slice sampling as proposed by Murray et al (2010). It was developed for models, where dependencies are generated through a latent multivariate normal distribution. In (SA), the AR(1) structure implies, that the vector $\mathbf{h}_{0:T} | \mu, \phi, \sigma$ has a $(T+1)$ dimensional multivariate normal distribution with mean vector $\boldsymbol{\mu}^{AR}$ and covariance matrix Σ^{AR} given by

$$\boldsymbol{\mu}^{AR} = \begin{pmatrix} \mu \\ \mu \\ \vdots \\ \mu \end{pmatrix} \in \mathbb{R}^{T+1}, \quad \Sigma^{AR} = \frac{\sigma^2}{1 - \phi^2} \begin{pmatrix} 1 & \phi & \phi^2 & \dots & \phi^T \\ \phi & 1 & \phi & \dots & \phi^{T-1} \\ \vdots & \vdots & \vdots & & \vdots \\ \phi^T & \phi^{T-1} & \phi^{T-2} & \dots & 1 \end{pmatrix} \in \mathbb{R}^{(T+1) \times (T+1)}. \quad (7)$$

(see e.g. Brockwell et al (2002), Chapter 2.2). The posterior density is given by

$$\left(\prod_{t=1}^T f(\mathbf{y}_t | h_t) \right) \varphi(\mathbf{h}_{0:T} | \boldsymbol{\mu}^{AR}, \Sigma^{AR}) \pi(\mu) \pi(\phi) \pi(\sigma),$$

where $\boldsymbol{\mu}^{AR}$ and Σ^{AR} are given in (7) and $\pi(\cdot)$ denotes the corresponding prior density as specified in (5). The initial state can be sampled from its full conditional density given by

$$f(h_0 | \mathbf{h}_{1:T}, \mu, \phi, \sigma) = \varphi(h_0 | \mu + \phi(h_1 - \mu), \sigma^2).$$

The full conditional density of the latent states $\mathbf{h}_{1:T}$ is given by

$$f(\mathbf{h}_{1:T} | Y, h_0, \mu, \phi, \sigma) \propto \left(\prod_{t=1}^T f(\mathbf{y}_t | h_t) \right) \varphi(\mathbf{h}_{1:T} | \boldsymbol{\mu}_{1:T|0}, \Sigma_{1:T|0}),$$

with a corresponding mean vector $\boldsymbol{\mu}_{1:T|0}$ and covariance matrix $\Sigma_{1:T|0}$. The mean vector and the covariance matrix of the conditional distribution are derived later in (8) in a more general way. We could reparameterize the model by $\mathbf{h}'_{1:T} = \mathbf{h}_{1:T} - \boldsymbol{\mu}_{1:T|0}$, to impose a multivariate normal prior with zero mean. We obtain the situation elliptical slice sampling was designed for. However updating the whole T dimensional vector $\mathbf{h}_{1:T}$ with elliptical slice sampling at once will lead to high autocorrelation in the posterior draws. This is illustrated in Section 3.3 and was also observed by Hahn et al (2016), where elliptical slice sampling was used for linear regression models. Hahn et al (2016) circumvent this problem by partitioning the vector $\mathbf{h}_{1:T}$ into smaller blocks. Such blocking strategies have also been employed by Shephard and Pitt (1997) and Watanabe and Omori (2004). We follow this approach and partition the set $\{1, \dots, T\}$ into m different blocks $B_1, \dots, B_m \subset \{1, \dots, T\}$. Let $a_i = \min_{s \in B_i} s$ denote the minimal and $b_i = \max_{s \in B_i} s$ denote the maximal index in the i -th block. The blocks are chosen such that $B_i = \{t \in \{1, \dots, T\} : a_i \leq t \leq b_i\}$, for $i = 1, \dots, m$. The full conditional density for the i -th block is given by $f(\mathbf{h}_{B_i} | Y, h_0, \mathbf{h}_{-B_i}, \mu, \phi, \sigma) \propto \left(\prod_{t \in B_i} f(\mathbf{y}_t | h_t) \right) f(\mathbf{h}_{B_i} | h_0, \mathbf{h}_{-B_i}, \mu, \phi, \sigma)$, where $-B_i = \{1, \dots, T\} \setminus B_i$. The vector $\mathbf{h}_{B_i} | h_0, \mathbf{h}_{-B_i}, \mu, \phi, \sigma$ is multivariate normal distributed with mean denoted by $\boldsymbol{\mu}_{B_i|}$ and covariance matrix $\Sigma_{B_i|}$ (see (8)) and therefore the full conditional density can be written as

$$f(\mathbf{h}_{B_i} | Y, h_0, \mathbf{h}_{-B_i}, \mu, \phi, \sigma) \propto \left(\prod_{t \in B_i} f(\mathbf{y}_t | h_t) \right) \varphi(\mathbf{h}_{B_i} | \boldsymbol{\mu}_{B_i|}, \Sigma_{B_i|}).$$

To sample the latent states of the i -th block \mathbf{h}_{B_i} from its full conditional we proceed as follows

- Set $\mathbf{h}'_{B_i} = \mathbf{h}_{B_i} - \boldsymbol{\mu}_{B_i|}$
- Draw \mathbf{h}'_{B_i} from the density

$$f(\mathbf{h}'_{B_i} | Y, h_0, \mathbf{h}_{-B_i}, \mu, \phi, \sigma) \propto \left(\prod_{t \in B_i} f(\mathbf{y}_t | h_t) \right) \varphi(\mathbf{h}'_{B_i} | \mathbf{0}, \Sigma_{B_i|}),$$

using elliptical slice sampling, where $\varphi(\mathbf{h}'_{B_i} | \mathbf{0}, \Sigma_{B_i|})$ is interpreted as the prior density for \mathbf{h}'_{B_i} .

- Set $\mathbf{h}_{B_i} = \mathbf{h}'_{B_i} + \boldsymbol{\mu}_{B_i|}$

Now we derive $\boldsymbol{\mu}_{B_i|}$ and $\Sigma_{B_i|}$. By the conditional independence assumptions of the AR(1) process and the way we defined the blocks B_1, \dots, B_m we obtain

$$\begin{aligned} f(\mathbf{h}_{B_i} | h_0, \mathbf{h}_{-B_i}, \mu, \phi, \sigma) &= f(\mathbf{h}_{B_i} | h_{a_i-1}, h_{b_i+1}, \mu, \phi, \sigma), \text{ for } i = 1, \dots, m-1, \text{ and} \\ f(\mathbf{h}_{B_m} | h_0, \mathbf{h}_{-B_m}, \mu, \phi, \sigma) &= f(\mathbf{h}_{B_m} | h_{a_m-1}, \mu, \phi, \sigma). \end{aligned}$$

Conditional on μ, ϕ and σ , the vector $(h_{a_i-1}, \mathbf{h}_{B_i}, h_{b_i+1})$ is multivariate normal distributed with mean vector $\boldsymbol{\mu}_{(a_i-1, B_i, b_i+1)}^{AR} \in \mathbb{R}^{s_i+2}$ and covariance matrix $\Sigma_{(a_i-1, B_i, b_i+1); (a_i-1, B_i, b_i+1)}^{AR} \in$

$\mathbb{R}^{(s_i+2) \times (s_i+2)}$, where s_i is the cardinality of B_i . Thus the vector $\mathbf{h}_{B_i}|h_{a_i-1}, h_{b_i+1}, \mu, \phi, \sigma$ follows a multivariate normal distribution with mean vector $\boldsymbol{\mu}_{B_i|}$ and covariance matrix $\Sigma_{B_i|}$ given by

$$\begin{aligned}\boldsymbol{\mu}_{B_i|} &= \boldsymbol{\mu}_{B_i}^{AR} + \Sigma_{B_i;(a_i-1, b_i+1)}^{AR} \frac{1 - \phi^2}{(1 - \phi^{2(s_i+1)})\sigma^2} \begin{pmatrix} 1 & -\phi^{s_i+1} \\ -\phi^{s_i+1} & 1 \end{pmatrix} \begin{pmatrix} h_{a_i-1} - \mu \\ h_{b_i+1} - \mu \end{pmatrix}, \\ \Sigma_{B_i|} &= \Sigma_{B_i;B_i}^{AR} - \Sigma_{B_i;(a_i-1, b_i+1)}^{AR} \frac{1 - \phi^2}{(1 - \phi^{2(s_i+1)})\sigma^2} \begin{pmatrix} 1 & -\phi^{s_i+1} \\ -\phi^{s_i+1} & 1 \end{pmatrix} \Sigma_{(a_i-1, b_i+1);B_i}^{AR}.\end{aligned}\tag{8}$$

The vector $\mathbf{h}_{B_m}|h_{a_m-1}, \mu, \phi, \sigma$ corresponding to the last block is multivariate normal distributed with mean vector $\boldsymbol{\mu}_{B_m|}$ and covariance matrix $\Sigma_{B_m|}$ obtained as

$$\begin{aligned}\boldsymbol{\mu}_{B_m|} &= \boldsymbol{\mu}_{B_m}^{AR} + \Sigma_{B_m;a_m-1}^{AR} \frac{1 - \phi^2}{\sigma^2} (h_{a_m-1} - \mu), \\ \Sigma_{B_m|} &= \Sigma_{B_m;B_m}^{AR} - \Sigma_{B_m;a_m-1}^{AR} \frac{1 - \phi^2}{\sigma^2} \Sigma_{a_m-1;B_m}^{AR}.\end{aligned}$$

We need to sample from $N(0, \Sigma_{B_i|})$ several times during elliptical slice sampling. Instead of working with the $s_i \times s_i$ covariance matrix $\Sigma_{B_i|}$ we can more efficiently sample from the s_i dimensional normal distribution by using the conditional independence assumptions of the AR(1) process. It holds that

$$\begin{aligned}f(\mathbf{h}_{B_i}|h_{a_i-1}, h_{b_i+1}, \mu, \phi, \sigma) &= \prod_{t=0}^{s_i-1} f(h_{a_i+t}|\mathbf{h}_{a_i-1:a_i+t-1}, h_{b_i+1}, \mu, \phi, \sigma) \\ &= \prod_{t=0}^{s_i-1} f(h_{a_i+t}|h_{a_i+t-1}, h_{b_i+1}, \mu, \phi, \sigma),\end{aligned}$$

where $f(h_{a_i+t}|h_{a_i+t-1}, h_{b_i+1}, \mu, \phi, \sigma)$ is the univariate normal density with mean

$$\mu_{a_i+t|a_i+t-1, b_i+1} = \frac{1}{1 - \phi^{2(s_i+1-t)}} \left((\phi - \phi^{2s_i+1-2t})(h_{a_i+t-1} - \mu) + (\phi^{s_i-t} - \phi^{s_i+2-t})(h_{b_i+1} - \mu) \right),$$

and variance

$$\sigma_{a_i+t|a_i+t-1, b_i+1}^2 = \frac{\sigma^2}{1 - \phi^2} \left(1 - \frac{1}{1 - \phi^{2(s_i+1-t)}} \left(\phi^2 - 2\phi^{2(s_i-t+1)} + \phi^{2(s_i-t)} \right) \right).$$

So we can sample $\mathbf{h}_{B_i} = (h_{a_i+t})_{t=0, \dots, s_i-1}$ conditioned on $h_{a_i-1}, h_{b_i+1}, \mu, \phi, \sigma$ recursively by

$$h_{a_i+t} \sim N(\mu_{a_i+t|a_i+t-1, b_i+1}, \sigma_{a_i+t|a_i+t-1, b_i+1}^2),$$

for $t = 0, \dots, s_i - 1$ and then $\mathbf{h}_{B_i} - \boldsymbol{\mu}_{B_i|}$ is a sample from $N(0, \Sigma_{B_i|})$.

2.2 Sampling of the constant parameters in the sufficient augmentation

In (SA) the observation equation only depends on $\mathbf{h}_{1:T}$ and is independent of the parameters μ, ϕ and σ . The parameters μ, ϕ and σ only depend on $\mathbf{h}_{0:T}$. This allows to use the same approach as in Kastner and Frühwirth-Schnatter (2014) to sample the parameters μ, ϕ and σ in (SA). We reparameterize the model such that proposals can be found using Bayesian linear regression. We define $\gamma = \mu(1 - \phi)$ and the state equation is given by

$$h_t = \gamma + \phi h_{t-1} + \sigma \eta_t,$$

where $\eta_t \sim N(0, 1)$. For fixed $\mathbf{h}_{0:T}$, this is a linear regression model with regression parameters γ, ϕ and variance σ^2 . Proposals for (μ, ϕ, σ) are found and accepted or rejected as described in Kastner and Frühwirth-Schnatter (2014) Section 2.4 (two block sampler).

2.3 Sampling of the constant parameters in the ancillary augmentation

To sample μ, ϕ and σ in (AA) we deploy an adaptive random walk Metropolis Hastings scheme as suggested by Garthwaite et al (2016), where tuning parameters are selected automatically using the Robbins Monro process (Robbins and Monro (1985)). For sampling, it is convenient to move to unconstrained parameter spaces which is achieved by the following transformations

$$s = \log(\sigma), \quad \xi = F_Z(\phi).$$

Here $F_Z(x) = \frac{1}{2} \log\left(\frac{1+x}{1-x}\right)$ is Fisher's Z transformation. The from (5) implied log prior densities for ξ and s are up to an additive constant given by

$$\begin{aligned} \log(\pi(\xi)) &\propto (a_\phi - 1) \log(F_Z^{-1}(\xi) + 1) + (b_\phi - 1) \log(1 - F_Z^{-1}(\xi)) + \log(1 - (F_Z^{-1}(\xi))^2) \\ \log(\pi(s)) &\propto -s - \frac{1}{2B_\sigma} \exp(2s) + 2s. \end{aligned}$$

The log posterior density in (AA) is proportional to

$$\begin{aligned} lp_{(AA)}(\mu, \xi, s, h_0, \tilde{\mathbf{h}}_{1:T}|Y) &\propto \sum_{t=1}^T \log\left(f(\mathbf{y}_t|h_t(\tilde{\mathbf{h}}_{1:T}, \mu, F_Z^{-1}(\xi), \exp(s)))\right) - \frac{1}{2} \sum_{t=1}^T \tilde{h}_t^2 \\ &\quad + \log\left(\varphi\left(h_0|\mu, \frac{\exp(s)^2}{1 - F_Z^{-1}(\xi)^2}\right)\right) + \log(\pi(\mu)) + \log(\pi(\xi)) + \log(\pi(s)). \end{aligned}$$

We sample (μ, ϕ, σ) in two blocks, one block for μ and one block for (ϕ, σ) .

Update for μ

To sample the mean parameter μ from its full conditional we propose a new state μ_{prop} in the r -th iteration of the MCMC procedure by

$$\mu_{prop} \sim N(\mu_{cur}, \sigma_{MH,\mu}^{r-1}),$$

where μ_{cur} is the current value for μ . The proposal μ_{prop} is accepted with probability

$$R = \exp\left(lp_{(AA)}(\mu_{prop}, \xi, s, h_0, \tilde{\mathbf{h}}_{1:T}|Y) - lp_{(AA)}(\mu_{cur}, \xi, s, h_0, \tilde{\mathbf{h}}_{1:T}|Y)\right)$$

and the scaling parameter $\sigma_{MH,\mu}^r$ is updated according to Garthwaite et al (2016) by

$$\log(\sigma_{MH,\mu}^r) = \log(\sigma_{MH,\mu}^{r-1}) + 4.058 \frac{(R - 0.44)}{r - 1}.$$

The scaling parameter is reduced, if the acceptance probability is larger than 0.44 and increased if the acceptance probability is smaller than 0.44. We target an average acceptance probability of 0.44, as recommended by Roberts et al (2001) for univariate random walk Metropolis Hastings. The constant 4.058 controls the step size and is chosen as suggested by Garthwaite et al (2016).

Joint update for ϕ and σ

In the r -th iteration, a two dimensional proposal (ξ_{prop}, s_{prop}) for (ξ, s) is obtained by

$$(\xi_{prop}, s_{prop})^t \sim N_2((\xi_{cur}, s_{cur})^t, \Sigma_{MH,\xi,s}^{r-1}),$$

where (ξ_{cur}, s_{cur}) are the current values. The proposal is accepted with probability

$$R = \exp\left(lp_{(AA)}(\mu, \xi_{prop}, s_{prop}, h_0, \tilde{\mathbf{h}}_{1:T}|Y) - lp_{(AA)}(\mu, \xi_{cur}, s_{cur}, h_0, \tilde{\mathbf{h}}_{1:T}|Y)\right).$$

For adapting the covariance matrix we follow a suggestion of Garthwaite et al (2016). Let I_n denote the n -dimensional identity matrix. We set $\Sigma_{MH,\xi,s}^r = I_2$ if $r < 100$ and

$$\Sigma_{MH,\xi,s}^r = (\sigma_{MH,\xi,s}^r)^2 \left(\hat{\Sigma}^r + \frac{(\sigma_{MH,\xi,s}^r)^2}{r} I_2 \right) \quad \text{if } r \geq 100.$$

Here $\hat{\Sigma}^r$ is the empirical covariance matrix of $(\xi^i, s^i)_{i=1,\dots,r}$, the first r samples for (ξ, s) , and

$$\log(\sigma_{MH,\xi,s}^r) = \log(\sigma_{MH,\xi,s}^{r-1}) + 6.534 \frac{(R - 0.234)}{r - 1}.$$

The matrix $\hat{\Sigma}^r + \frac{(\sigma_{MH,\xi,s}^r)^2}{r} I_2$ is a positive definite estimate of the covariance matrix. This covariance estimate is scaled by $(\sigma_{MH,\xi,s}^r)^2$ to obtain the covariance matrix for the proposal in the next iteration. The scaling $(\sigma_{MH,\xi,s}^r)^2$ is tuned to achieve an average acceptance probability of 0.234 as suggested by Roberts et al (1997) for multivariate random walk Metropolis Hastings. To reduce computational cost the empirical covariance matrix $\hat{\Sigma}^r$ can be updated in every step by the following recursion (see e.g. Bennett et al (2009))

$$\hat{\Sigma}^r = \frac{r-2}{r-1} \hat{\Sigma}^{r-1} + \frac{1}{r} ((\xi^r, s^r)^t - \hat{\mu}^{r-1})((\xi^r, s^r)^t - \hat{\mu}^{r-1})^t,$$

where $\hat{\mu}^{r-1}$ is the sample mean of $(\mu^i, \xi^i)_{i=1,\dots,r-1}$. We also update the sample mean recursively by

$$\hat{\mu}^r = \frac{1}{r} ((r-1)\hat{\mu}^{r-1} + (\xi^r, s^r)^t).$$

3 Illustration of the proposed sampler

We illustrate the MCMC sampler we proposed in the previous section for three established models. We consider the dynamic bivariate copula model of Almeida and Czado (2012), the stochastic volatility model with Gaussian errors (Kim et al (1998)) and the stochastic volatility model with skew Student t errors (Abanto-Valle et al (2015)). For the implementation of the sampler we used `Rcpp` (Eddelbuettel et al (2011)) which allows to embed C++ code into R. In addition we make use of `rvinecopulib` (Nagler and Vatter (2018)) to evaluate copula densities and of `RcppEigen` (Bates et al (2013)). For sampling (μ, ϕ, σ) in (SA) as described in Section 2.2 we use corresponding parts of the implementation of the R package `stochvol` (Kastner (2016a)).

3.1 The stochastic volatility model with Gaussian errors

We simulate $T = 500$ observations from the stochastic volatility model as given in (3) with parameters $\mu = -10$, $\phi = 0.9$ and $\sigma = 0.3$. Then we apply the sampler developed in Section 2 with blocks of size 5. We obtain 26000 draws and discard the first 1000 for burn in. Figure 1 shows trace plots and estimated posterior densities for the parameters μ, ϕ, σ and h_{200} . These plots and the effective sample sizes shown in Table 1 indicate that the chain mixes well.

μ	ϕ	σ	h_{200}
9127.28	617.97	500.32	4705.50

Table 1: Effective sample sizes for the parameters μ, ϕ, σ and h_{200} of the stochastic volatility model.

3.2 The stochastic volatility model with skew Student t errors

The stochastic volatility model with skew Student t errors is obtained by replacing the normal distribution of the stochastic volatility model of the previous section by a skew Student t

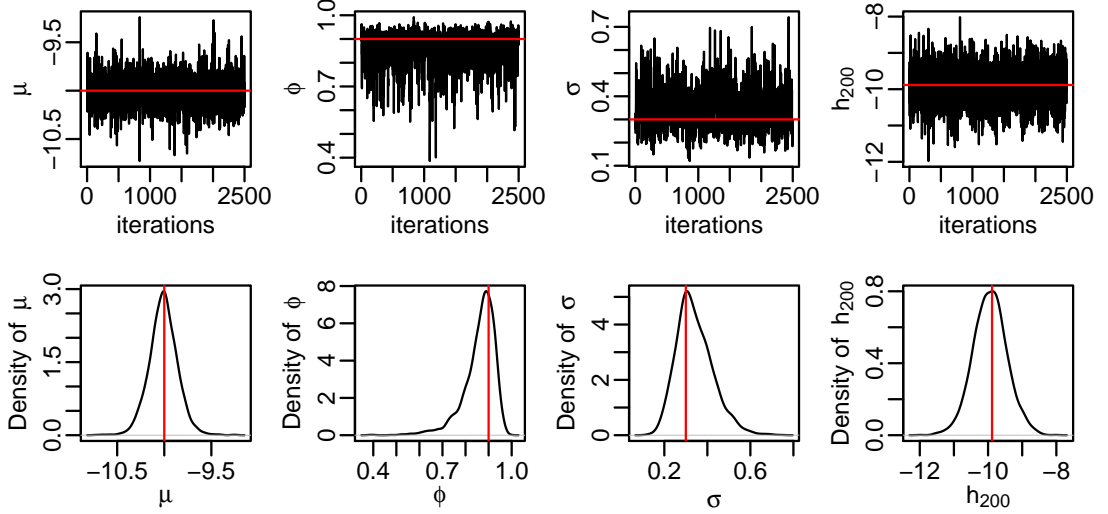


Figure 1: Traceplots and estimated posterior densities based on 2500 MCMC draws after a burn in of 1000 and thinning with factor 10 for the parameters μ , ϕ , σ and h_{200} of the stochastic volatility model. True values are added in red.

distribution. This allows for heavy tails and skewness. The stochastic volatility model with skew Student t errors as considered by Abanto-Valle et al (2015) is given by

$$\begin{aligned} Y_t &= \exp\left(\frac{h_t}{2}\right)\epsilon_t \\ h_t &= \mu + \phi(h_{t-1} - \mu) + \sigma\epsilon_t, \end{aligned} \quad (9)$$

where $\epsilon_t \sim sst(\epsilon_t|\alpha, df)$ independently for $t = 1, \dots, T$. We denote by $sst(\epsilon_t|\alpha, df)$ the density of the standardized skew Student t distribution with parameters $\alpha \in \mathbb{R}$ and $df > 2$ (cf. Appendix A). Compared to our framework this model has two additional parameters α and df . For these additional parameters we choose the following prior distributions

$$\alpha \sim N(0, 10), \quad df \sim N_{>2}(5, 5), \quad (10)$$

where $N_{>2}$ denotes the normal distribution truncated to $(2, \infty)$. We need to ensure that $df > 2$ since the standardized skew Student t distribution would not be well defined otherwise.

Conditional on α and df our sampler can be applied directly to sample $(\mu, \phi, \sigma, \mathbf{h}_{0:T})$ from its full conditional. Another approach, which lead to better mixing, is to include the parameters α and df in the interweaving strategy. The sampler is slightly modified in the following way:

- a) Sample $\mathbf{h}_{0:T}$ from $\mathbf{h}_{0:T}|Y, \mu, \phi, \sigma, \alpha, df$.
- b) Sample $(\mu, \phi, \sigma, \alpha, df)$ in (SA) from $\mu, \phi, \sigma, \alpha, df|Y, \mathbf{h}_{0:T}$.
- c) Move to (AA) via $\tilde{h}_t = \frac{h_t - \mu - \phi(h_{t-1} - \mu)}{\sigma}$, for $t = 1, \dots, T$.
- d) Sample $(\mu, \phi, \sigma, \alpha, df)$ in (AA) from $\mu, \phi, \sigma, \alpha, df|Y, h_0, \tilde{\mathbf{h}}_{1:T}$.
- e) Move back to (SA) via the recursion $h_t = \mu + \phi(h_{t-1} - \mu) + \sigma\tilde{h}_t$ for $t = 1, \dots, T$.

For step a) we proceed as described in Section 2.1. For step b) we draw (μ, ϕ, σ) from its full conditional as described in Section 2.2. The parameters α and df are drawn from its univariate full conditional distribution using adaptive Metropolis Hastings using similar arguments as in Section 2.3. For step d) we investigated different blocking strategies for the parameters $(\mu, \phi, \sigma, \alpha, df)$. We compared the different strategies with respect to effective sample sizes and decided to use the following three blocks: (μ, df) , (ϕ, σ) and α . Each block is updated using adaptive Metropolis Hastings similar to Section 2.3.

μ	ϕ	σ	h_{200}	α	df
2087.60	519.47	291.43	2525.84	869.90	761.71

Table 2: Effective sample sizes for the parameters μ , ϕ , σ , h_{200} , α and df of the stochastic volatility model with skew Student t errors.

For illustration we simulate $T = 500$ observations from the stochastic volatility model with skew Student t errors with parameters $\mu = -10$, $\phi = 0.95$, $\sigma = 0.3$, $\alpha = 2$ and $df = 4$. We run the sampler with blocks of size 5 for 26000 iterations and discard the first 1000 for burn in. The trace plots and estimated posterior densities for the parameters μ , ϕ , σ , α and df are shown in Figure 2. We conclude from these plots and from the effective sample sizes, shown in Table 2, that the chain mixes well.

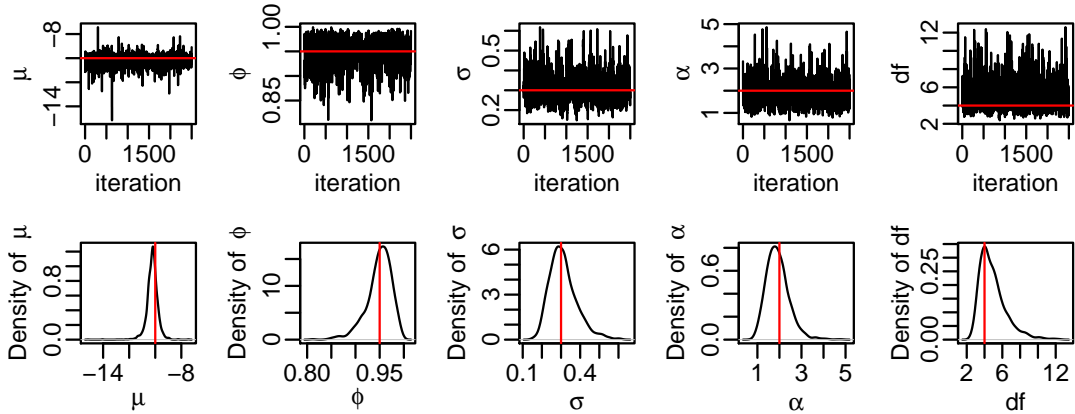


Figure 2: Traceplots and estimated posterior densities based on 2500 MCMC draws after a burn in of 1000 and thinning with factor 10 for the parameters μ , ϕ , σ , α and df of the stochastic volatility model with skew Student t errors. True values are added in red.

3.3 Dynamic bivariate copula models

Kastner and Frühwirth-Schnatter (2014) have already shown that interweaving improves sampling efficiency a lot for the stochastic volatility model. Here, we demonstrate that interweaving can also lead to better mixing for the dynamic bivariate copula model of Almeida and Czado (2012).

We simulate from the dynamic bivariate copula model of Almeida and Czado (2012) as given in (4) two times with different parameter specifications as shown in Table 3. The chosen copula family is an extended Clayton copula, which extends the Clayton copula to allow for negative Kendall's τ values. More precisely, the extended Clayton copula has the following density

$$c(u_1, u_2; \theta) = \begin{cases} c_{Clayton}(u_1, u_2, \theta) & \text{if } \theta \geq 0 \\ c_{Clayton}(1 - u_1, u_2, -\theta) & \text{if } \theta < 0, \end{cases}$$

where $c_{Clayton}(\cdot, \cdot; \theta)$ is the density of the bivariate Clayton copula with parameter θ (see Joe (2014), Chapter 4). So the extended Clayton copula is equal to the Clayton copula for non negative Kendall's τ and equal to a 90 degree rotation of the Clayton copula for negative Kendall's τ .

We use the sampler developed in Section 2 with blocks of size 5 and run it for 26000 iterations, where the first 1000 are discarded for burn in. We refer to this sampler with interweaving and blocking as the standard sampler. To illustrate the necessity of the steps in the proposed sampling procedure we run two other samplers. The following three samplers are considered:

- **Standard:** interweaving and blocking
- **No interweaving:** blocking and no interweaving

- **No blocking:** interweaving and no blocking, i.e. the latent states $\mathbf{h}_{1:T}$ are updated jointly.

For comparison we have a look at trace plots of 2500 draws after a burn in of 1000 and thinning with factor 10 in Figure 3. Additional plots of the estimated posterior densities are shown in the supplementary material. We observe that all three samplers produce posterior samples covering the true values. The trace plots suggest that the standard sampler achieves better mixing. This can also be seen from effective sample sizes as shown in Table 3.

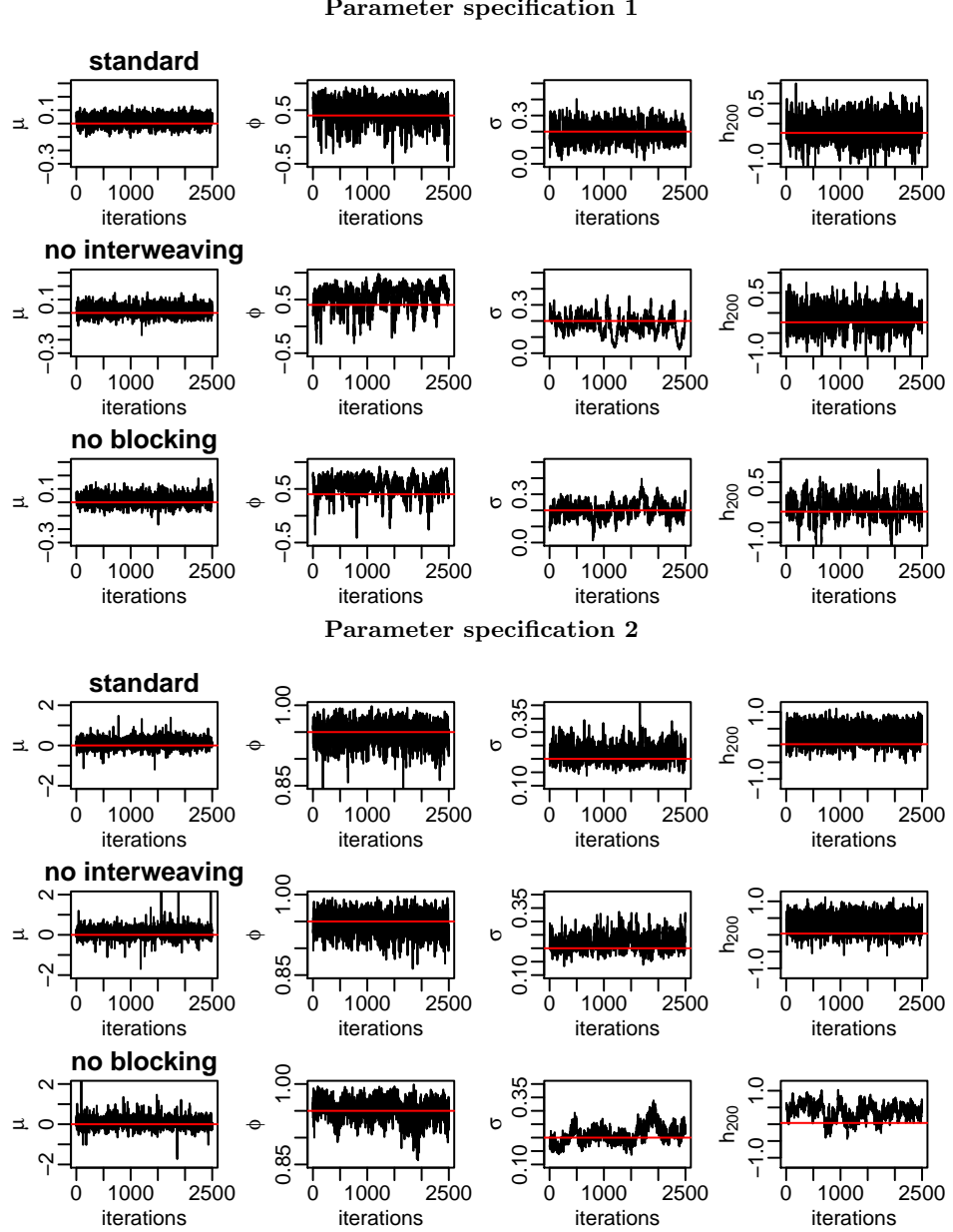


Figure 3: Traceplots of 2500 MCMC draws after a burn in of 1000 and thinning with factor 10 for parameter specifications 1 and 2 of the dynamic bivariate copula model. We show traceplots for the parameters μ , ϕ , σ and h_{200} for the standard sampler, the sampler with no interweaving and the sampler with no blocking. True values are added in red.

Parameter specification 1		μ	ϕ	σ	h_{200}
true parameters		0	0.4	0.2	
effective sample size	standard	4634.77	475.10	376.29	2880.52
	no interweaving	1455.31	114.80	46.32	1445.31
	no blocking	711.14	104.78	73.65	112.07
Parameter specification 2					
true parameters		0	0.95	0.2	
effective sample size	standard	4511.34	783.84	373.33	4782.60
	no interweaving	3246.23	778.87	255.89	2468.17
	no blocking	2596.43	223.47	32.60	49.18

Table 3: Effective sample sizes based on 25000 posterior draws after a burn in of 1000 for the parameters μ , ϕ , σ and h_{200} for the three different samplers for parameter specifications 1 and 2 of the dynamic bivariate copula model.

4 A dynamic bivariate mixture copula model for time varying asymmetric tail dependence

Dependence among financial assets is often modeled with a Student t copula. This copula allows for tail dependence symmetric in the upper and lower tail. Evidence against the assumption of symmetric tail dependence has been provided and models to handle this characteristic have become necessary (Patton (2006), Nikolouloupoulos et al (2012), Jondeau (2016)). Patton (2006) proposes the symmetrized Joe-Clayton copula. This is a modification of the BB7 copula (Joe (2014), Chapter 4) that is symmetric if upper and lower tail dependence coincide, which he describes as a desirable property. In the application of Nikolouloupoulos et al (2012) the Student t copula provides the best fit in terms of the likelihood. But they argue that if the focus is on the tails a BB1 or BB7 copula might be more appropriate. The BB1 and BB7 copulas have two parameters which might not be enough, if we want to model three characteristics in a flexible way: upper tail dependence, lower tail dependence and overall dependence as measured with Kendall's τ . We provide another approach to relax the symmetric tail dependence assumption. We propose a mixture of a Student t and a extended Gumbel copula with parameters $\tau \in (-1, 1)$, $\nu > 2$ and $p \in [0, 1]$ given by

$$C^M(u_1, u_2; \tau, \nu, p) = pC^t(u_1, u_2; \tau, \nu) + (1 - p)C^G(u_1, u_2; \tau), \quad (11)$$

where C^t is the bivariate Student t copula specified by Kendall's τ and the degree of freedom ν and C^G is the bivariate extended Gumbel copula specified by Kendall's τ . The extended Gumbel copula is defined similarly to the extended Clayton copula in Section 3.3, i.e. it is equal to the Gumbel copula for positive values of Kendall's τ and equal to a 90 degree rotation of the Gumbel copula for negative Kendall's τ values. Both copulas C^t and C^G share the dependence parameter τ and we expect the mixture copula to have a similar strength of dependence. The corresponding Kendall's τ of the mixture copula is given by

$$\begin{aligned} \tau^M &= \int_{(0,1)^2} C^M(u_1, u_2; \tau, \nu, p) c^M(u_1, u_2; \tau, \nu, p) du_1 du_2 = (p^2 + (1 - p)^2) \tau + \\ &+ \int_{(0,1)^2} p(1 - p) (C^G(u_1, u_2; \tau))(c^t(u_1, u_2; \tau, \nu) + C^t(u_1, u_2; \tau, \nu)c^G(u_1, u_2; \tau)) du_1 du_2. \end{aligned} \quad (12)$$

We evaluated the integral in (12) numerically for different values of τ , p and ν and observed only negligible difference between τ and τ^M . The upper and lower tail dependence coefficients

λ_M^L and λ_M^U of the mixture copula can, for $\tau > 0$, be obtained as

$$\begin{aligned}\lambda_M^L(\tau, p, \nu) &= \lim_{u \rightarrow 0} \frac{C^M(u, u)}{u} = \lim_{u \rightarrow 0} \frac{pC^t(u_1, u_2; \tau, \nu) + (1-p)C^G(u_1, u_2; \tau)}{u} \\ &= p2T_{\nu+1}\left(-\sqrt{\frac{(\nu+1)(1-\sin(\frac{\pi\tau}{2}))}{1+\sin(\frac{\pi\tau}{2})}}\right) + 0 \\ \lambda_M^U(\tau, p, \nu) &= p2T_{\nu+1}\left(-\sqrt{\frac{(\nu+1)(1-\sin(\frac{\pi\tau}{2}))}{1+\sin(\frac{\pi\tau}{2})}}\right) + (1-p)(2-2^{1-\tau}),\end{aligned}$$

where we used the well known formulas for the tail dependence coefficients of the Student t and the Gumbel copula (Joe (2014), Chapter 4). Whereas the upper and lower tail dependence coefficients measure dependence in the upper right and lower left corner, we are also interested in the dependence in the upper left and the lower right corner when $\tau < 0$. We consider the following tail dependence coefficients in the upper left corner λ_M^{UL} and in the lower right corner λ_M^{LR} if $\tau < 0$

$$\lambda_M^{LR} = \lambda_M^L(-\tau, p, \nu), \quad \lambda_M^{UL} = \lambda_M^U(-\tau, p, \nu),$$

analogous to the definition of quarter tail dependence in Fink et al (2017).

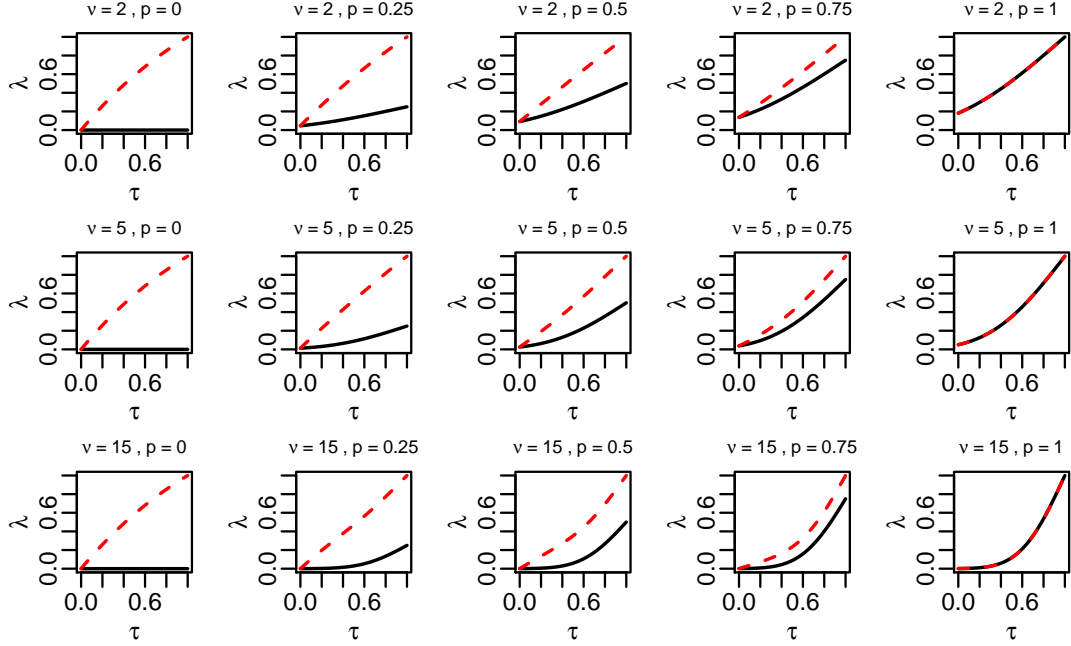


Figure 4: Upper (red, dashed) and lower (black) tail dependence coefficient of the mixture copula defined in (11) plotted against Kendall's τ for different values of ν and p .

The tail dependence coefficient of the mixture copula is a linear combination of the tail dependence coefficients of its two components, the Student t and the Gumbel copula. The Student t copula has symmetric tail dependence, whereas the Gumbel copula has upper but no lower tail dependence. So we expect upper tail dependence to be higher than lower tail dependence in the mixture copula. The amount of asymmetry in the tails is controlled by p , whereas the copula is symmetric in the tails for $p = 1$ and the level of asymmetry increases as we decrease p . So this copula allows for great flexibility: The overall dependence can be described by Kendall's τ , the degrees of freedom parameter controls the upper and lower tail dependence coefficient and p controls the difference between upper and lower tail dependence. This is visualized in Figure 4. Note that the desirable property according to Patton (2006) of symmetry in case of coinciding upper and lower tail dependence is here fulfilled. If we expected higher lower than upper tail dependence we can replace the Gumbel copula by a survival Gumbel

copula which has the density $c^{SG}(u_1, u_2) = c^G(1 - u_1, 1 - u_2)$. In Figure 5, the mixture copula defined in (11) is visualized with normalized contour plots, i.e. for $(U_1, U_2) \sim C^M(\cdot, \cdot; \tau, \nu, p)$ we consider the contour plot of $(Z_1, Z_2) = (\Phi^{-1}(U_1), \Phi^{-1}(U_2))$. Here Φ is the standard normal distribution function.

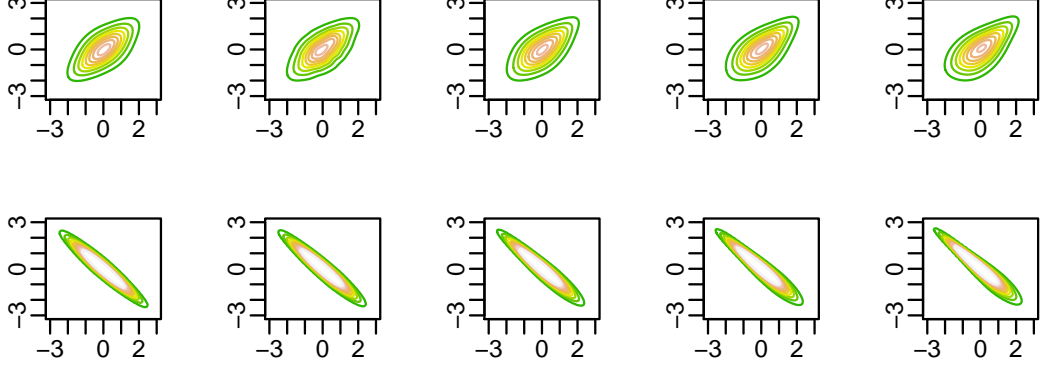


Figure 5: Normalized contour plots for the mixture copula model in (11) with $\tau = 0.4$ (top row), $\tau = -0.8$ (bottom row), $\nu = 5$ and $p = 1, 0.75, 0.5, 0.25, 0$ (from left to right).

To allow for time variation we use the mixture copula C^M of (11) within the dynamic bivariate copula model of Almeida and Czado (2012). A non linear state space model for T bivariate random vectors $(U_{t1}, U_{t2})_{t=1, \dots, T} \in [0, 1]^{T \times 2}$, corresponding to T time points, is given by

$$\begin{aligned} (U_{t1}, U_{t2}) &\sim c^M(u_{t1}, u_{t2}; \tau_t, \nu, p) \text{ independently} \\ h_t &= \mu + \phi(h_{t-1} - \mu) + \sigma \epsilon_t, \end{aligned} \quad (13)$$

for $t = 1, \dots, T$, where $h_t = F_Z(\tau_t)$ and the other parameters are defined similarly to (4). We assign a uniform prior on $[0, 1]$ for p , a normal prior with mean 5 and standard deviation 20 truncated to the interval $(2, \infty]$ for ν and the same priors as in (5) for the remaining parameters. Sampling is done in the following way.

- Draw $\log\left(\frac{p}{1-p}\right)$ and $\log(\nu - 2)$ from its univariate full conditionals with random walk Metropolis Hastings with Gaussian proposal (proposal standard deviation: 0.3).
- Draw $\mu, \phi, \sigma, h_0, \dots, h_T$ conditioned on p and ν as in Section 3.3.

To illustrate this sampling procedure we simulate 500 observations from the model defined in (13) with parameters $p = 0.6, \nu = 5, \mu = 0.1, \phi = 0.95$ and $\sigma = 0.2$. We run the sampler for 26000 iterations and discard the first 1000 iterations as burn in. Effective sample sizes are shown in Table 4. They suggest that the sampling procedure works reasonable. This is supported by trace plots and estimated posterior densities (supplementary material). In Figure 6 we see that our sampler recovers the simulated dynamics.

μ	ϕ	σ	h_{200}	ν	p
4442.72	762.20	296.12	4411.21	415.79	393.52

Table 4: Effective sample sizes for several parameters of the dynamic bivariate mixture copula model.

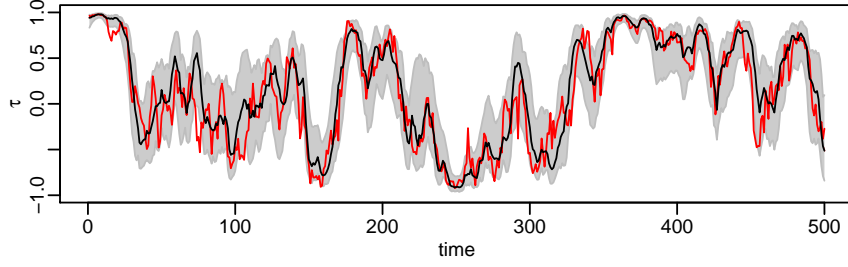


Figure 6: Posterior mode estimates of Kendall's τ for the dynamic bivariate mixture copula model are plotted against time t . The 5% and 95% posterior quantiles construct a 90% credible interval added in grey. The true (simulated) values for Kendall's τ are added in red.

5 Application: Modeling the volatility return relationship

The two step copula modeling approach motivated by Sklar's theorem (Sklar (1959)) provides a very flexible method for the construction of multivariate distributions. We can combine arbitrary marginal distributions with any copula. In the financial context, we propose a bivariate model that combines the skew Student t stochastic volatility model of Section 3.2 for the margins with the dynamic mixture copula we introduced in Section 4. This model allows for asymmetry and heavy tails in the marginal distribution as well as for time varying asymmetric tail dependence in the dependence structure. More precisely, we assume that for T bivariate random vectors $(Y_{t1}, Y_{t2})_{t=1, \dots, T} \in \mathbb{R}^{T \times 2}$ the following holds

$$(Y_{t1}, Y_{t2}) \sim C^M \left(ssT \left(\frac{y_{t1}}{\exp(h_{t1}^{st}/2)} \middle| \alpha_1^{st}, df_1^{st} \right), ssT \left(\frac{y_{t2}}{\exp(h_{t2}^{st}/2)} \middle| \alpha_2^{st}, df_2^{st} \right); F_Z^{-1}(h_t^{cop}), \nu^{cop}, p^{cop} \right) \quad (14)$$

independently, where

$$\begin{aligned} h_{tj}^{st} &= \mu_j^{st} + \phi_j^{st}(h_{t-1;j}^{st} - \mu_j^{st}) + \sigma_j^{st} \epsilon_{tj}^{st} \\ h_t^{cop} &= \mu^{cop} + \phi^{cop}(h_{t-1}^{cop} - \mu^{cop}) + \sigma^{cop} \epsilon_t^{cop} \end{aligned}$$

and $\epsilon_{tj}^{st}, \epsilon_t^{cop} \sim N(0, 1)$ iid, α_j^{st}, df_j^{st} as in (10), ν^{cop}, p^{cop} as in (13) and $\mu_j^{st}, \mu^{cop}, \phi_j^{st}, \phi^{cop}, \sigma_j^{st}, \sigma^{cop}, h_{0j}^{st}, h_0^{cop}$ as in (2) and (5) for $j = 1, 2$ and $t = 1, \dots, T$. Here, ssT denotes the distribution function of the standardized skew Student t distribution (cf. Appendix A). We refer to the transforms $ssT(y_{t1} \exp(-h_{t1}^{st}/2) | \alpha_1^{st}, df_1^{st})$ and $ssT(y_{t2} \exp(-h_{t2}^{st}/2) | \alpha_2^{st}, df_2^{st})$ for $t = 1, \dots, T$ as udata.

With this model, we investigate the volatility return relationship through the bivariate joint distribution of a stock index and the corresponding volatility index. The joint distribution of return and volatility incorporates all the marginal information as well as information about the dependence, which are both relevant for hedging and risk management (Allen et al (2012)). Since there has already been evidence for asymmetry in the joint distribution of volatility and return (Allen et al (2012), Fink et al (2017)) our model might be a good candidate for this application.

For inference we rely on a two step approach. We first estimate marginal distributions and based on these estimates we estimate the copula parameters. This approach is also called inference for margins (Joe and Xu (1996)) and is commonly used in copula modeling. Due to its advantages, also many Bayesian researchers rely on a two step approach for copula models (Min and Czado (2011), Almeida and Czado (2012), Smith (2015), Gruber et al (2015), Loaiza-Maya et al (2018)). Here, the likelihood consists of a product of the marginal densities and the copula density $c^M(u_1, u_2, \theta)$. In our case all three arguments u_1, u_2, θ of the copula are modeled dynamically. We obtained high values for the copula density by choosing high dependence and scale u_1, u_2 appropriately with their dynamical marginal variances. This scaling of the

variances may increase the copula contribution to the likelihood, while decreasing the marginal contribution. Thus different parameter choices may lead to similar values of the likelihood. Such multimodal posterior distributions are difficult to estimate in general. Furthermore this lead to results that do not seem reasonable. For example we observed udata deviating far from being marginally uniformly distributed and very high oscillations in the latent log variances. Although oscillations are supposed to be controlled by the AR(1) prior, we have seen that the effect in the likelihood outweighs the effect of the prior. This shows that a joint Bayesian estimation approach for this setup might run into problems. In a two step approach, $\mathbf{h}_{1:T;j}^{st}$ is estimated only based on data $\mathbf{y}_{1:T;j}$ ($j = 1, 2$) and the above-mentioned problems can be circumvented. Furthermore the two step approach allows for faster inference by dividing the problem into smaller parts, which converge faster. In addition to that, the calculation of udata several times in every step, as required by a fully Bayesian approach, is here avoided. This is particularly important here since we require expensive evaluations of the standardized skew Student t distribution function. Given these reasons we restrict ourselves to a two step approach.

We consider the S&P500 (SPX) and its volatility index the VIX as well as the DAX and its volatility index the VDAX. The daily log returns from 2006 to 2013 of these indices are obtained from Yahoo finance (<https://finance.yahoo.com>). With approximately 250 trading days per year this results in 2063 observations, visualized in Figure 12 in Appendix B. The corresponding data matrix with 2063 rows and 4 columns is denoted by \mathbf{Y} .

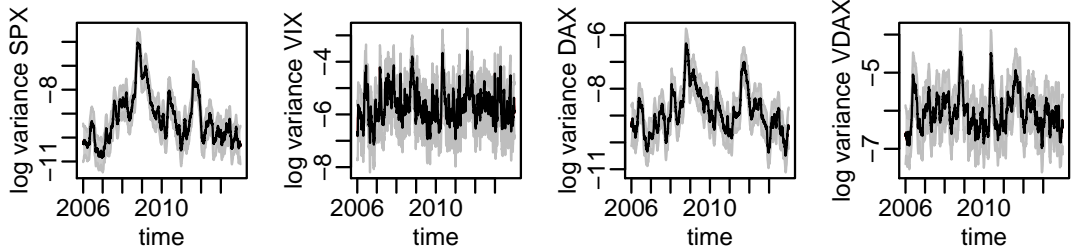


Figure 7: Posterior mode estimates of the daily log variances of the four skew Student t stochastic volatility models for the indices SPX, VIX, DAX, VDAX from 2006 to 2013 plotted against time. The 90% credible region, added in grey, is constructed from the 5% and 95% posterior quantiles.

First we fit a skew Student t stochastic volatility model for each of the indices as described in Section 3.2. For each index we run 26000 iterations and discard the first 1000 as burn in. As it is typical for financial data all indices show a high persistence parameter ϕ (Posterior mode estimates for ϕ : SPX: 0.99, VIX: 0.89, DAX: 0.99, VDAX: 0.96). A notable difference is that for stock indices we observe negative skewness, whereas for the volatility indices positive skewness is observed (Posterior mode estimates for α : SPX: -0.51 , VIX: 1.33, DAX: -0.48 , VDAX: 0.99). Evidence for negative skewness has also been observed for the log returns of other stock indices, as e.g., for the NASDAQ by Abanto-Valle et al (2015). Posterior mode estimates, posterior quantiles and effective samples sizes for several parameters of the four marginal models are summarized in Table 8 in the Appendix. The estimated daily log variances are shown in Figure 7. In the end of 2009, the estimated variances are high for all indices due to the financial crisis.

In the next step we obtain pseudo copula data on the (0,1) scale by applying the probability integral transform using the posterior mode estimates of the marginal parameters. We refer to this data as pseudo udata and it is obtained as

$$u_{tj} = ssT \left(y_{tj} \exp \left(-\frac{\hat{h}_{tj}^{st}}{2} \right); \hat{\alpha}_j^{st}, \hat{df}_j^{st} \right),$$

where $\hat{h}_{tj}^{st}, \hat{\alpha}_j^{st}, \hat{df}_j^{st}$ are the posterior mode estimates of the corresponding marginal skew Student t stochastic volatility model for $t = 1, \dots, T, j = 1, \dots, 4$. In the udata marginal characteristics are removed and what is left is information about the dependence structure. For a first visual

analysis of the dependence structure we consider marginally normalized contour plots for the pair (SPX,VIX) and the pair (DAX,VDAX) for different time periods in Figure 8. These shapes indicate asymmetry in the tails. To analyse time variation in the dependence, we estimate Kendall's τ at time point t as the empirical Kendall's τ of the 50 observations before and after time point t . This is visualized in Figure 9. These indications for time varying and asymmetric dependence motivate the use of the dynamic mixture copula model. Two of these models are fitted based on the pseudo udata, one corresponding to the pair (SPX,VIX) and one corresponding to the pair (DAX,VDAX). We run the sampler for 26000 iterations, where the first 1000 are discarded as burn in. The posterior mode estimates for p are 0.29 for the model for (SPX,VIX) and 0.64 for the model for (DAX,VDAX), respectively. (Further, posterior statistics for the model parameters μ, ϕ, σ, p and ν are shown in Table 7 in the Appendix). So both fitted models allow for asymmetric tail dependence, whereas the asymmetry is stronger for the (SPX,VIX) model. For these models tail dependence in the upper left corner λ_M^{UL} is stronger than the one in the lower right corner λ_M^{LR} . This means that joint extreme comovements, where the stock index decreases and the volatility index increases are more likely to occur than vice versa.

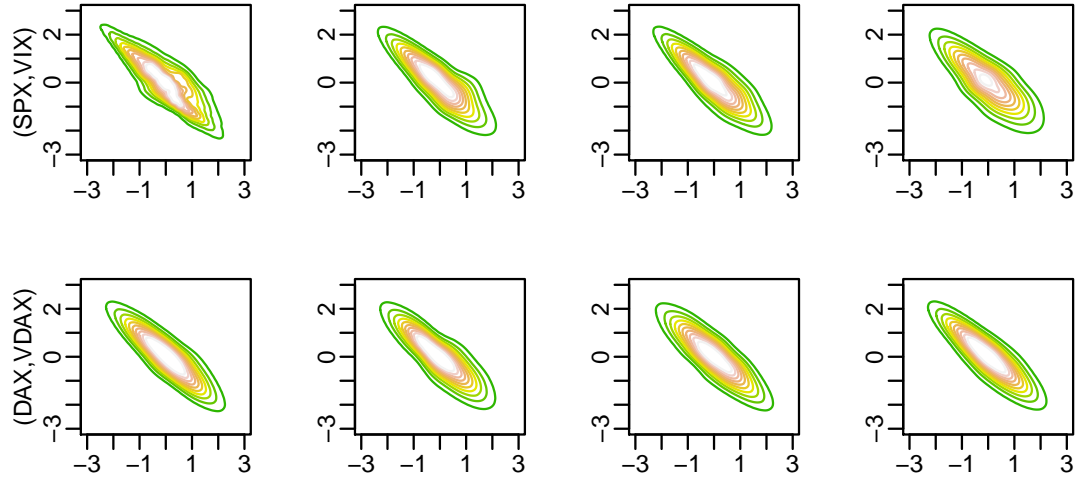


Figure 8: Normalized contour plots corresponding to the pairs (SPX, VIX) (top row) and the pair (DAX,VDAX) (bottom row) calculated for four different periods. The periods are obtained by dividing the whole time period of length 2063 into four parts of approximately equal length 500.

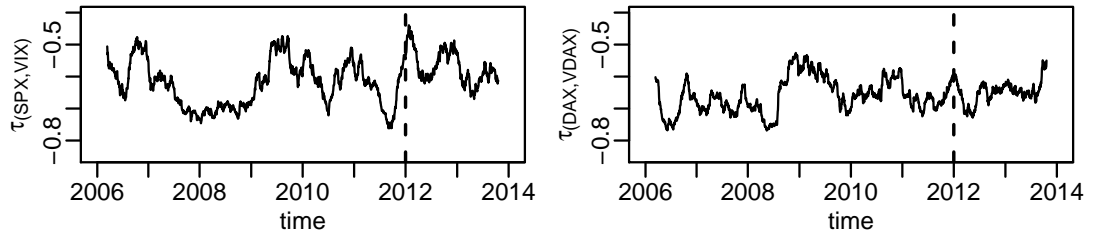


Figure 9: Rolling window estimates of Kendall's τ (Kendall's τ at time t is estimated as empirical Kendall's τ based on the 50 observations before and after time t). The left plot shows the estimated Kendall's τ of the pair (SPX, VIX) and the right plot of the pair (DAX,VDAX). Observations after the dashed line belong to the test set.

The time varying estimates for Kendall's τ and the tail dependence coefficients are shown in Figure 10. The figure visualizes the asymmetry in tail dependence. We also observe changes

in tail dependence as time evolves: for (SPX,VIX), λ_M^{UL} ranges from 0.43 to 0.72 and λ_M^{LR} from 0.003 to 0.09. For the pair (DAX,VDAX), λ_M^{UL} ranges from 0.14 to 0.68 and λ_M^{LR} from 0.003 to 0.35. This variation over time in tail dependence goes hand in hand with variation in Kendall's τ . For (SPX,VIX), Kendall's τ ranges from -0.75 to -0.47 and for (DAX,VDAX) from -0.79 to -0.31 .

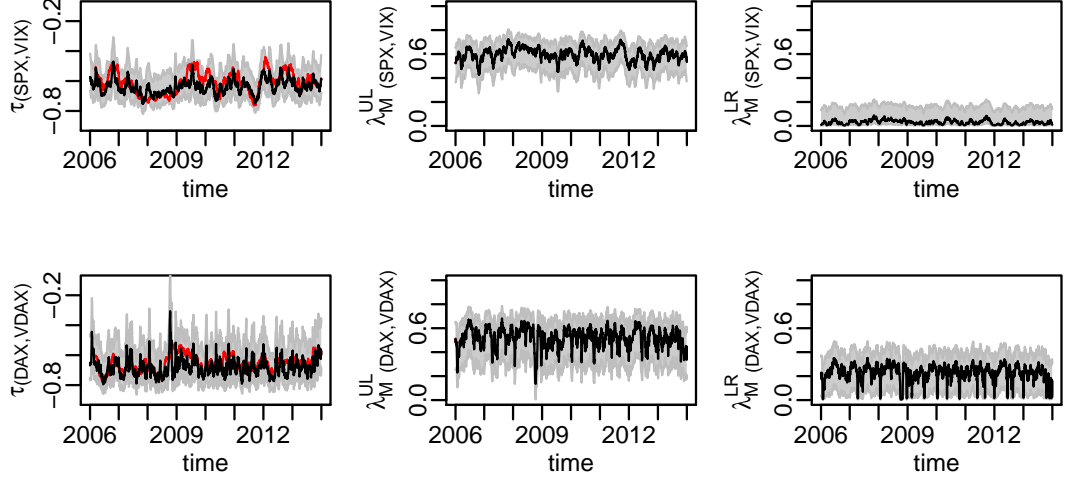


Figure 10: In these plots the top row corresponds to the pair (SPX, VIX), the bottom row to the pair (DAX,VDAX). The first column shows posterior mode estimates of Kendall's τ , where the Kendall's τ obtained from rolling window estimates (also shown in Figure 9) is added in red. The middle column shows posterior mode estimates of λ_M^{UL} and the right column shows estimates of λ_M^{LR} . Credible regions, constructed from the 5% and 95% posterior quantiles, are added in grey.

We aim to further support the findings we obtained through the dynamic copula model, i.e. that the dependence structure is asymmetric and varies over time. Therefore we consider several restrictions with respect to the dependence structure. Giving up time variation leads to a constant mixture copula, giving up asymmetry leads to a dynamic Student t copula and giving up time variation and asymmetry leads to a constant Student t copula. In addition, we compare our model to the frequently used dynamic conditional correlation (DCC) GARCH model of Engle (2002). The DCC-GARCH allows for time varying symmetric dependence. So we take five different models into consideration. These models are summarized in Table 5. The model \mathcal{M}_{dyn}^{mix} is the model given in (14), which was also used for the previous analysis.

model	specification	margin	dependence	
		asymmetric	asymmetric	dynamic
\mathcal{M}_{dyn}^{mix}	sstSV + dynamic mixture copula	Yes	Yes	Yes
$\mathcal{M}_{const}^{mix}$	sstSV + constant mixture copula	Yes	Yes	No
\mathcal{M}_{dyn}^t	sstSV + dynamic Student t copula	Yes	No	Yes
\mathcal{M}_{const}^t	sstSV + constant Student t copula	Yes	No	No
\mathcal{M}_{DCC}	DCC(1,1)-GARCH(1,1)	No	No	Yes

Table 5: Different models considered for comparison. Models are specified by: marginal model + copula model. The skew Student t stochastic volatility model as given in (9) is denoted by sstSV. The mixture copula is defined in (11). If a copula is dynamic, the corresponding copula is considered within the dynamic bivariate copula model framework of Almeida and Czado (2012) given in (4).

We compare the models with respect to cumulative log predictive likelihoods. Log predictive

likelihoods are commonly used for this task (Kastner (2016b), Bitto and Frühwirth-Schnatter (2018)) and form a strictly proper scoring rule (Gneiting and Raftery (2007)). In comparison to other multivariate scoring rules, such as the energy score or the variogram score (Scheuerer and Hamill (2015)), log predictive likelihoods have here the advantage that they can be computed fast since they require only one evaluation of the predictive density per observation. Since our predictive likelihoods are based on point estimates, Kastner (2016b) refers to them as pseudo log predictive likelihoods in contrast to log predictive likelihoods, where the predictive density is obtained by integrating out the unknown parameters.

We consider $T + K$ observations of dimension two, stored in the data matrix $Y_{1:(T+K);1:2}$, where the first T observations are used to train the model and the last K are used for testing.

The DCC-GARCH model is estimated based on T data points in the training period. Based on this model, we obtain rolling one day ahead estimates of the covariance matrix for each day in the test set. The log predictive likelihoods are obtained by evaluating the corresponding multivariate normal densities at the observations. To estimate the DCC-GARCH models we used the R package `rmgarch` of Ghalanos (2012).

Similarly, the model \mathcal{M}_{dyn}^{mix} is estimated with the training data. Instead of computing daily updates for all model parameters we fix the constant parameters at their posterior mode estimates to save computation time. The dynamic parameters are updated daily and the one day ahead forecasts are obtained by evolving the AR(1) process. To obtain the log predictive likelihood we evaluate the density implied by (14) at the corresponding observations. Appendix B contains a detailed description of this procedure. The cumulative log predictive likelihoods for $\mathcal{M}_{const}^{mix}$, \mathcal{M}_{dyn}^t and \mathcal{M}_{const}^t are obtained similarly.

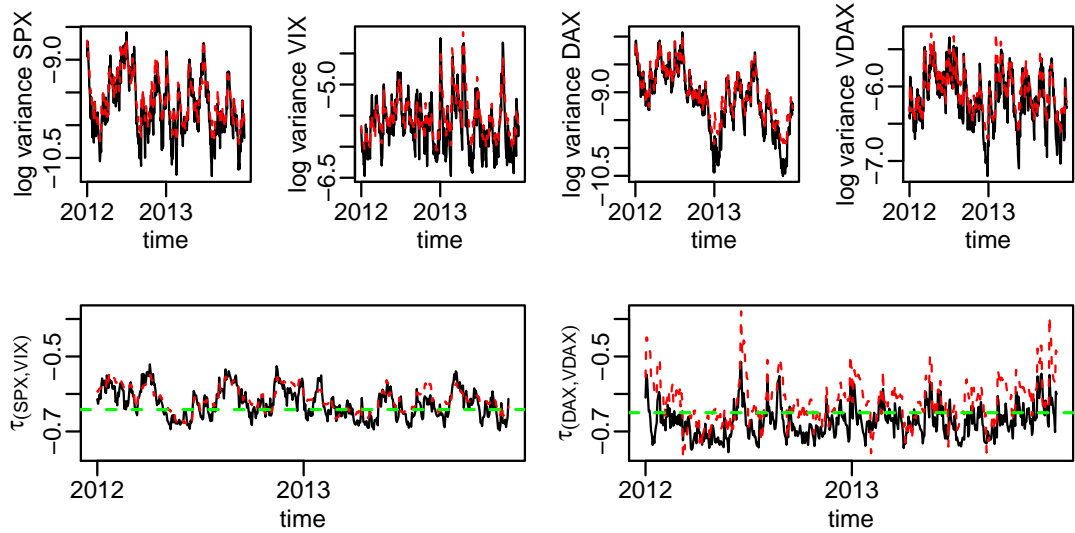


Figure 11: The top row shows the one day ahead predicted log variance for each day in 2012 - 2013 for the models \mathcal{M}_{dyn}^{mix} (black) and \mathcal{M}_{DCC} (dashed, red). The bottom row shows one day ahead predicted Kendall's τ for each day in 2012 - 2013 for the models \mathcal{M}_{dyn}^{mix} (black), $\mathcal{M}_{const}^{mix}$ (dashed, green) and \mathcal{M}_{DCC} (dashed, red). Note that the predictions of the log variances coincide for the models $\mathcal{M}_{const}^{mix}$ and \mathcal{M}_{dyn}^{mix} .

This procedure for calculating the log predictive likelihood is applied for both data sets corresponding to the pairs (SPX, VIX) and (DAX, VDAX). We evaluated the log predictive density for every trading day in the last two years (2012 - 2013) of our data set, which yields $K = 517$. As training period we use $T = 1000$ which corresponds to a training period of approximately four years. When evaluating the log predictive likelihoods we also obtain predicted variances and predicted Kendall's τ values. Figure 11 shows the one day ahead predicted log variances and Kendall's τ values for the models \mathcal{M}_{dyn}^{mix} , $\mathcal{M}_{const}^{mix}$ and \mathcal{M}_{DCC} . The models \mathcal{M}_{dyn}^{mix} and $\mathcal{M}_{const}^{mix}$ both use a skew Student t stochastic volatility model for the margins and therefore the predictions for the marginal log variances coincide. In comparison to the GARCH margins, the

stochastic volatility margins allow for bigger oscillations with respect to the predicted variance. Table 6 summarizes the cumulative log predictive likelihoods. In both cases, for the (SPX,VIX) as well as for the (DAX,VDAX) data, the best model is provided by the dynamic mixture copula model \mathcal{M}_{dyn}^{mix} . Furthermore, we see that in both cases the constant mixture copula model $\mathcal{M}_{const}^{mix}$ is preferred over the constant and dynamic Student t copula models \mathcal{M}_{const}^t and \mathcal{M}_{dyn}^t . For the (DAX,VDAX) data, the second best model is provided by the constant mixture copula model $\mathcal{M}_{const}^{mix}$. For this data the rolling window estimates of Kendall's τ in Figure 9 vary less than for the (SPX,VIX) data. For the (SPX,VIX) data, the DCC-GARCH \mathcal{M}_{DCC} yields the second best log predictive likelihoods.

	\mathcal{M}_{dyn}^{mix}	$\mathcal{M}_{const}^{mix}$	\mathcal{M}_{dyn}^t	\mathcal{M}_{const}^t	\mathcal{M}_{DCC}
(SPX,VIX)	2743.4	2734.3	2733.8	2726.6	2737.2
(DAX,VDAX)	2818.2	2812.1	2807.4	2807.3	2789.0

Table 6: Cumulative log predictive likelihoods for the models \mathcal{M}_{dyn}^{mix} , $\mathcal{M}_{const}^{mix}$, \mathcal{M}_{dyn}^t , \mathcal{M}_{const}^t and \mathcal{M}_{DCC} .

6 Conclusion

We propose a sampler, applicable to general non linear state space models with univariate autoregressive state equation. Sampling efficiency is demonstrated for several established models. Furthermore we use the sampler to estimate the parameters of a dynamic bivariate mixture copula model. This mixture copula model turns out to be a candidate to model the volatility return relationship, since in our application it produces more accurate forecasts than a bivariate DCC-GARCH model or a Student t copula model.

In this work, there are two objectives that might be extended: The sampler and the bivariate mixture copula model. The sampler could be extended to allow for a broader class of models. For example we might consider autoregressive processes of higher order in the state equation. In this case we can still rely on elliptical slice sampling and on an interweaving strategy. Another extension could relax the assumption of a Gaussian dependence structure in the state equation by replacing the autoregressive process by a D-vine copula model. In this case elliptical slice sampling can no longer be applied to sample the latent states and an alternative sampling method is required.

The bivariate dynamic mixture copula could serve as a building block for regular vine copula models. Thus we could extend the bivariate model to arbitrary dimensions. This is interesting if we study not only the bivariate volatility return relationship, but for example the dependence structure among several exchange rates.

Acknowledgment

The second author is supported by the German Research Foundation (DFG grant CZ 86/4-1). Computations were performed on a Linux cluster supported by DFG grant INST 95/919-1 FUGG.

Appendix A. The standardized skew Student t distribution

According to Azzalini and Capitanio (2003), the density of the univariate skew Student t distribution with parameters $\xi \in \mathbb{R}$, $\omega \in (0, \infty)$, $\alpha \in \mathbb{R}$ and $df \in (0, \infty)$ is given by

$$st(x|\xi, \omega, \alpha, df) = \frac{2}{\omega} t(x|df) T \left(\alpha \frac{x - \xi}{\omega} \sqrt{\frac{df + 1}{\left(\frac{x - \xi}{\omega}\right)^2 + df}} \middle| df + 1 \right),$$

where $t(\cdot|df)$ is the density function of the univariate Student t distribution with df degrees of freedom and $T(\cdot|df)$ the corresponding distribution function. The expectation and variance of

a random variable X following a skew Student t distribution with parameters ξ, ω, α as above and $df > 2$ are given by

$$E(X) = \xi + \omega b_{df} \delta, \text{ and } Var(X) = \omega^2 \left(\frac{df}{df-2} - b_{df}^2 \delta^2 \right),$$

where $\delta = \frac{\alpha^2}{\sqrt{1+\alpha^2}}$ and $b_{df} = \sqrt{\frac{df}{\pi} \frac{\Gamma(\frac{df-1}{2})}{\Gamma(\frac{df}{2})}}$. If we set

$$\omega = \sqrt{\frac{1}{\left(\frac{df}{df-2} - b_{df}^2 \delta^2\right)}} \text{ and } \xi = -\omega b_{df} \delta = -\sqrt{\frac{1}{\left(\frac{df}{df-2} - b_{df}^2 \delta^2\right)}} b_{df} \delta,$$

only the parameters α and df remain unknown and the random variable has zero mean and a variance of one. We refer to the corresponding distribution as the standardized skew Student t distribution. Its density is denoted by sst and is obtained as

$$sst(x|\alpha, df) = st \left(x \middle| -\sqrt{\frac{1}{\left(\frac{df}{df-2} - b_{df}^2 \delta^2\right)}} b_{df} \delta, \sqrt{\frac{1}{\left(\frac{df}{df-2} - b_{df}^2 \delta^2\right)}}, \alpha, df \right). \quad (15)$$

Appendix B. Additional material for Section 5 (Application)

Daily log returns

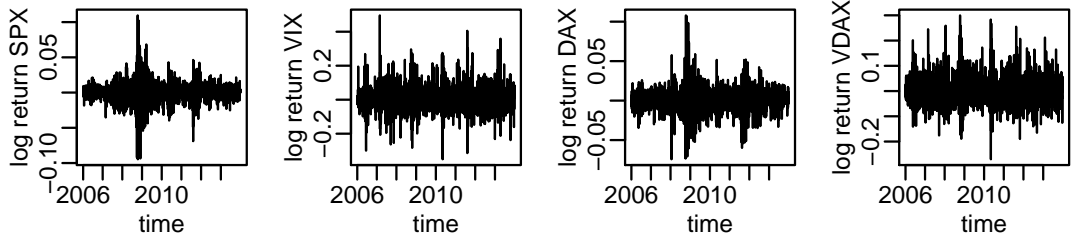


Figure 12: Daily log returns of the four indices SPX, VIX, DAX, VDAX from 2006 to 2013 plotted against time.

Posterior statistics

	mode	5% quantile	95% quantile	effective sample size
(SPX,VIX)				
μ	-0.74	-0.77	-0.71	1610.98
ϕ	0.93	0.83	0.96	205.15
σ	0.05	0.03	0.09	173.87
p	0.29	0.11	0.42	855.55
ν	8.66	5.11	41.61	897.51
(DAX,VDAX)				
μ	-0.81	-0.84	-0.78	1824.87
ϕ	0.85	0.73	0.92	255.58
σ	0.10	0.06	0.13	169.03
p	0.64	0.48	0.78	1776.19
ν	7.61	5.70	33.75	558.82

Table 7: Posterior mode estimates, posterior quantiles and effective sample sizes for the dynamic mixture copula models for the pairs (SPX,VIX) and (DAX,VDAX).

	mode	5% quantile	95% quantile	effective sample size
SPX				
μ	-9.29	-9.95	-8.68	13455.45
ϕ	0.99	0.98	1.00	486.07
σ	0.15	0.12	0.19	174.02
α	-0.51	-0.78	-0.22	4370.85
df	6.66	5.37	10.22	1468.80
VIX				
μ	-5.65	-5.80	-5.50	2979.96
ϕ	0.89	0.84	0.93	367.33
σ	0.36	0.29	0.48	288.54
α	1.33	0.97	1.73	897.35
df	9.00	6.62	15.23	1030.40
DAX				
μ	-8.89	-9.29	-8.50	14957.44
ϕ	0.99	0.97	0.99	541.34
σ	0.15	0.13	0.19	277.12
α	-0.48	-0.80	-0.06	4925.88
df	9.65	7.38	14.90	2256.84
VDAX				
μ	-6.06	-6.22	-5.89	6343.39
ϕ	0.96	0.92	0.97	378.46
σ	0.18	0.13	0.24	277.55
α	0.99	0.66	1.28	3006.30
df	8.35	6.43	12.85	1451.69

Table 8: Posterior mode estimates, posterior quantiles and effective sample sizes for the univariate skew Student t stochastic volatility models for the four indices SPX, VIX, DAX, VDAX.

Calculating the log predictive likelihood

We describe in detail how we proceed for model \mathcal{M}_{dyn}^{mix} . We consider $T + K$ observations of dimension two, stored in the data matrix $Y_{1:(T+K);1:2}$, where the first T observations are used to train the model and the last K are used for evaluation.

Step 1: (Model fitting based on the training period)

- We fit two marginal skew Student t stochastic volatility models to $\mathbf{y}_{1:T;1}$ and $\mathbf{y}_{1:T;2}$. This yields R_{train} draws of the parameters denoted by $\mathbf{h}_{1:T;j}^{st,r}$, $\mu_j^{st,r}$, $\phi_j^{st,r}$, $\sigma_j^{st,r}$, $\alpha_j^{st,r}$ and $df_j^{st,r}$, $r = 1, \dots, R_{train}$ and corresponding posterior mode estimates $\hat{\mathbf{h}}_{1:T;j}^{st}$, $\hat{\mu}_j^{st}$, $\hat{\phi}_j^{st}$, $\hat{\sigma}_j^{st}$, $\hat{\alpha}_j^{st}$ and \hat{df}_j^{st} for $j = 1, 2$.
- We estimate the udata

$$u_{tj} = ssT \left(y_{tj} \exp \left(-\frac{\hat{h}_{tj}^{st}}{2} \right) \middle| \hat{\alpha}_j^{st}, \hat{df}_j^{st} \right)$$

for $t = 1, \dots, T, j = 1, 2$.

- We fit the dynamic bivariate mixture copula model introduced in (13) based on the udata $U_{1:T;1:2}$ and obtain posterior draws $\mathbf{h}_{1:T}^{cop,r}$, $\mu^{cop,r}$, $\phi^{cop,r}$, $\sigma^{cop,r}$, $\nu^{cop,r}$, $p^{cop,r}$ for $r = 1, \dots, R_{train}$ and corresponding posterior mode estimates $\hat{\mathbf{h}}_{1:T}^{cop}$, $\hat{\mu}^{cop}$, $\hat{\phi}^{cop}$, $\hat{\sigma}^{cop}$, $\hat{\nu}^{cop}$, \hat{p}^{cop} .

Step 2: (The one day ahead predictive density)

Estimating the one day ahead predictive density at time $T + k, 1 \leq k \leq K$ would usually require to fit daily models with observations up to time $T + k - 1$ for $k = 1, \dots, K$. In order to save computational resources we use another approach where we only update the dynamic

parameters, i.e. the log variances and Kendall's τ . For the constant parameters we use the estimates from the training period $1, \dots, T$. In this case we found that it is enough to only consider a time horizon of 100 time points, i.e. to estimate a dynamic parameter at time $T+k$ we consider data in the period $T+k-100, \dots, T+k-1$. We proceed as follows to obtain the one day ahead predictive density at time point $T+k$ with $1 \leq k \leq K$.

- We consider a skew Student t stochastic volatility model as in (9), where we keep the parameters $\mu, \phi, \sigma, \alpha$ and df fixed and only update the latent log variances. Therefore we draw the latent log variances $\mathbf{h}_{(T+k-100):(T+k-1);j}^{st}$ conditional on $\mathbf{y}_{(T+k-100):(T+k-1);j}$, $\hat{\mu}_j^{st}, \hat{\phi}_j^{st}, \hat{\sigma}_j^{st}, \hat{df}_j^{st}$ and $\hat{\alpha}_j^{st}$ for $j = 1, 2$. We denote the draws by $\mathbf{h}_{(T+k-100):(T+k-1);j}^{st,r}$, $r = 1, \dots, R_{test}$ for $j = 1, 2$. Corresponding posterior mode estimates are denoted by $\hat{\mathbf{h}}_{(T+k-100):(T+k-1);j}^{st}$, $j = 1, 2$.
- We estimate the udata via the probability integral transform, i.e. for $j = 1, 2$ and $t = T+k-100, \dots, T+k-1$ we calculate

$$u_{tj} = ssT \left(y_{tj} \exp \left(-\frac{\hat{h}_{tj}^{st}}{2} \right) \middle| \hat{\alpha}_j^{st}, \hat{df}_j^{st} \right).$$

- We fit the dynamic mixture copula model to the udata $U_{(T+k-100):(T+k-1);(1:2)}$ where we keep the constant parameters fixed. We only update $\mathbf{h}_{(T+k-100):(T+k-1)}^{cop}$ conditional on $U_{(T+k-100):(T+k-1);(1:2)}, \hat{\mu}^{cop}, \hat{\phi}^{cop}, \hat{\sigma}^{cop}, \hat{\nu}^{cop}, \hat{p}^{cop}$. The corresponding draws are denoted by $\mathbf{h}_{(T+k-100):(T+k-1)}^{cop,r}$, $r = 1, \dots, R_{test}$ and the posterior mode estimates by $\hat{\mathbf{h}}_{(T+k-100):(T+k-1)}^{cop}$.
- For $j = 1, 2$, we obtain an estimate for the log variance at time point $T+k$ as $\hat{h}_{T+k;j}^{st} = \hat{\mu}_j^{st} + \hat{\phi}_j^{st}(\hat{h}_{T+k-1;j}^{st} - \hat{\mu}_j^{st})$.
- We obtain an estimate for Fisher's Z transform of Kendall's τ at time point $T+k$, as $\hat{h}_{T+k}^{cop} = \hat{\mu}^{cop} + \hat{\phi}^{cop}(\hat{h}_{T+k-1}^{cop} - \hat{\mu}^{cop})$.
- The predictive density evaluated at (y_1, y_2) is given by

$$f_{T+k}^p(y_1, y_2) = c_{T+k}^p(y_1, y_2) g_{T+k}^p(y_1, y_2),$$

with

$$c_{T+k}^p(y_1, y_2) = c^M \left(ssT \left(x_1 \middle| \hat{\alpha}_1^{st}, \hat{df}_1^{st} \right), ssT \left(x_2 \middle| \hat{\alpha}_2^{st}, \hat{df}_2^{st} \right); F_Z^{-1}(\hat{h}_{T+k}^{cop}), \hat{\nu}^{cop}, \hat{p}^{cop} \right),$$

where c^M is the density of the mixture copula defined in (11) and

$$g_{T+k}^p(y_1, y_2) = sst \left(x_1 \middle| \hat{\alpha}_1^{st}, \hat{df}_1^{st} \right) sst \left(x_2 \middle| \hat{\alpha}_2^{st}, \hat{df}_2^{st} \right) \exp \left(-\frac{\hat{h}_{T+k;1}^{st}}{2} \right) \exp \left(-\frac{\hat{h}_{T+k;2}^{st}}{2} \right),$$

with $x_j = y_j \exp \left(-\frac{\hat{h}_{T+k;j}^{st}}{2} \right)$ for $j = 1, 2$.

Step 3: (The cumulative log predictive likelihood)

The cumulative log predictive likelihood is obtained as

$$LP = \sum_{k=1}^K \log(f_{T+k}^p(y_{T+k;1}, y_{T+k;2})).$$

During the training period we run $R_{train} = 26000$ iterations with a burn in of 1000, while for updating only the dynamic parameters 11000 iterations with a burn in of 1000 is enough, i.e. we use $R_{test} = 11000$.

Supplement

Elliptical slice sampling

We assume that the posterior density for a parameter vector θ given data D is given by

$$f(\theta|D) \propto \ell(\theta|D)\varphi(\theta|0, \Sigma), \quad (16)$$

where $\ell(\theta|D)$ is the likelihood function and $\varphi(\theta|0, \Sigma)$ is the multivariate normal density with zero mean and covariance matrix Σ . Murray et al (2010) consider the Metropolis Hastings sampler of Neal (1998) where a proposal θ' is obtained from the following stochastic representation

$$\theta' = \sqrt{1 - \alpha^2}\theta + \alpha v, v \sim N(0, \Sigma). \quad (17)$$

Here $\alpha \in [-1, 1]$ is a fixed step size parameter. The proposal is accepted with probability

$$\min\left(1, \frac{\ell(\theta')}{\ell(\theta)}\right). \quad (18)$$

Elliptical slice sampling adapts the step size parameter α during sampling. This eliminates the need to select the parameter before sampling and it may be a better approach for situations where good choices of the step size parameter depend on the region of the state space. Murray et al (2010) first suggest alternatively to propose a new state by

$$\theta' = \cos(\omega)\theta + \sin(\omega)v, v \sim N(0, \Sigma). \quad (19)$$

Here the angle ω corresponds to the step size. As we move ω towards zero the proposal gets closer to the initial value θ . Murray et al (2010) argue that (19) provides a more flexible choice for the proposals compared to (17), if the parameter ω is also updated, which is here the case. In elliptical slice sampling we first draw an angle ω from the uniform distribution on $[0, 2\pi]$ and obtain a proposal as outlined in (19). This proposal is accepted according to (18). If the proposal is not accepted a new angle is selected with a slice sampling approach (Neal (2003)) such that the angle approaches zero as more samples are rejected. This ensures that at some point the proposal will be accepted. The approach is outlined in Algorithm 1. Murray et al (2010) show that this samples from a Markov chain, where (16) is the corresponding stationary distribution.

Algorithm 1 Elliptical slice sampling

```

1:  $v \sim N(0, \Sigma)$ 
2:  $u \sim \text{uniform}(0, 1)$ 
3:  $\omega \sim \text{uniform}(0, 2\pi)$ 
4:  $\omega_{min} = \omega - 2\pi, \omega_{max} = \omega$ 
5:  $\theta' = \cos(\omega)\theta + \sin(\omega)v$ 
6: while  $\frac{\ell(\theta')}{\ell(\theta)} \leq u$  do
7:   if  $\omega < 0$  then
8:      $\omega_{min} = \omega$ 
9:   else
10:     $\omega_{max} = \omega$ 
11:   end if
12:    $\omega \sim \text{uniform}(\omega_{min}, \omega_{max})$ 
13:    $\theta' = \cos(\omega)\theta + \sin(\omega)v$ 
14: end while
```

The DCC-GARCH model

The DCC-GARCH model was introduced by Engle (2002). Mathematical properties were developed by Engle and Sheppard (2001). In the DCC-GARCH model it is assumed that a d dimensional random vector $r_t \in \mathbb{R}^d$ at time t is multivariate normal distributed with zero mean dynamic covariance matrix $H_t \in \mathbb{R}^{d \times d}$, i.e.

$$r_t \sim N(0, H_t),$$

for $t = 1, \dots, T$. The covariance matrix can be written as

$$H_t = D_t R_t D_t,$$

where R_t is a $d \times d$ correlation matrix and D_t is a $d \times d$ diagonal matrix. The diagonal matrix D_t contains the marginal standard deviations. We assume GARCH(P_j, Q_j) innovations for the j -th diagonal entry of D_t , i.e.

$$d_{t,j}^2 = \omega_j + \sum_{p=1}^{P_j} \alpha_{pj} r_{t-p,j}^2 + \sum_{q=1}^{Q_j} \beta_{qj} d_{t-q,j}^2,$$

where

- $\omega_j > 0$,
- $d_{t,0} > 0$,
- $\sum_{p=1}^{P_j} \alpha_{jp} + \sum_{q=1}^{Q_j} \beta_{qj} < 1$ and the roots of $1 - \sum_{p=1}^{P_j} \alpha_{jp} Z^p + \sum_{q=1}^{Q_j} \beta_{qj} Z^q$ lie outside the unit circle,
- α_{jp} for all $p \in \{1, \dots, P_j\}$ and β_{jq} for all $q \in \{1, \dots, Q_j\}$ are such that $d_{t,j}^2$ is positive.

The correlation matrix is decomposed as follows

$$R_t = \text{diag}(Q_t)^{-1/2} Q_t \text{diag}(Q_t)^{-1/2},$$

where Q_t is a positive definite matrix. Further we denote by

$$\epsilon_t = D_t^{-1} r_t$$

the standardized return and by \bar{Q} the estimated covariance matrix of the standardized returns obtained as

$$\bar{Q} = \sum_{t=1}^T \epsilon_t \epsilon_t^t.$$

For Q_t we assume the following dynamic structure

$$Q_t = (1 - \sum_{m=1}^M a_m - \sum_{n=1}^N b_n) \bar{Q} + \sum_{m=1}^M a_m \epsilon_{t-m} \epsilon_{t-m}^t + \sum_{n=1}^N b_n Q_{t-n},$$

where

- $a_m \geq 0$ for all $m \in \{1, \dots, M\}$ and $b_n \geq 0$ for all $n \in \{1, \dots, N\}$
- $\sum_{m=1}^M a_m + \sum_{n=1}^N b_n < 1$
- Q_0 is positive definite

Engle and Sheppard (2001) show that under the above conditions H_t is a proper covariance matrix. The DCC(M,N)-GARCH(P,Q) model is obtained by setting $P_j = P$ and $Q_j = Q$ for $j = 1, \dots, d$.

Further results for dynamic bivariate copula models

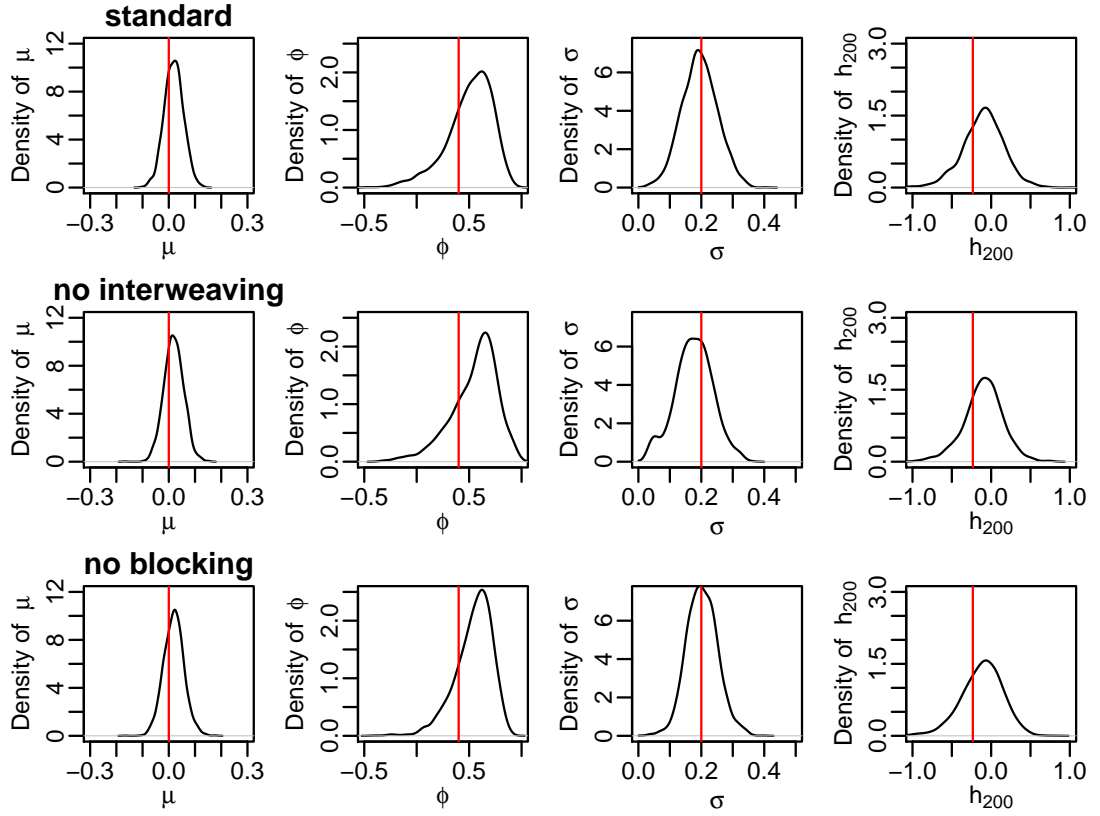


Figure 13: Estimated posterior density based on 2500 MCMC draws after a burn in of 1000 and thinning with factor 10 for parameter specification 1 of the dynamic bivariate copula model. We show the estimated posterior density for the parameters μ, ϕ, σ and h_{200} for the standard sampler (top row), the sampler with no interweaving (middle row) and the sampler with no blocking (bottom row). True values are added in red.

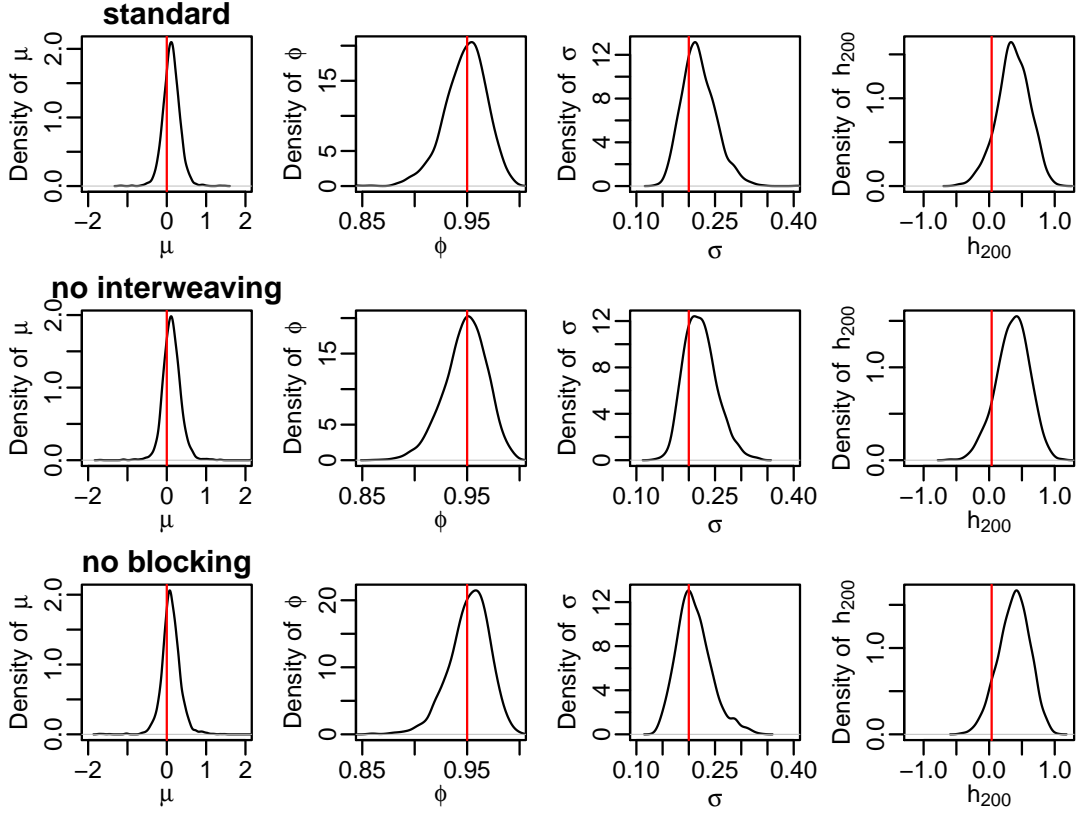


Figure 14: Estimated posterior density based on 2500 MCMC draws after a burn in of 1000 and thinning with factor 10 for parameter specification 2 of the dynamic bivariate copula model. We show the estimated posterior density for the parameters μ, ϕ, σ and h_{200} for the standard sampler (top row), the sampler with no interweaving (middle row) and the sampler with no blocking (bottom row). True values are added in red.

Further results for the dynamic mixture copula

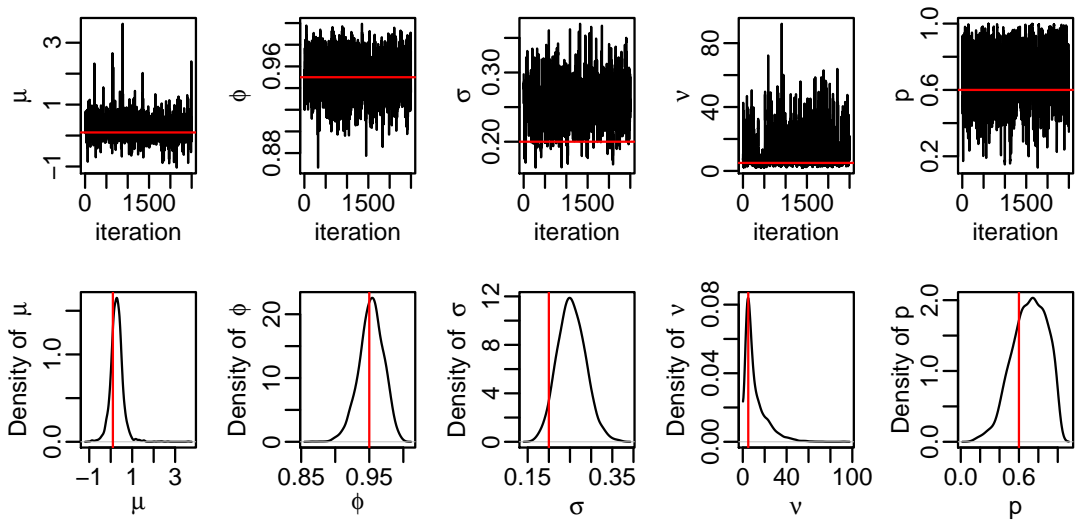


Figure 15: Traceplots and estimated posterior densities based on 2500 MCMC draws after a burn in of 1000 and thinning with factor 10 for the dynamic bivariate mixture copula model. We show traceplots and estimated posterior densities for the parameters μ, ϕ, σ, ν and p . True values are added in red.

Further results for the application

Results for the marginal models

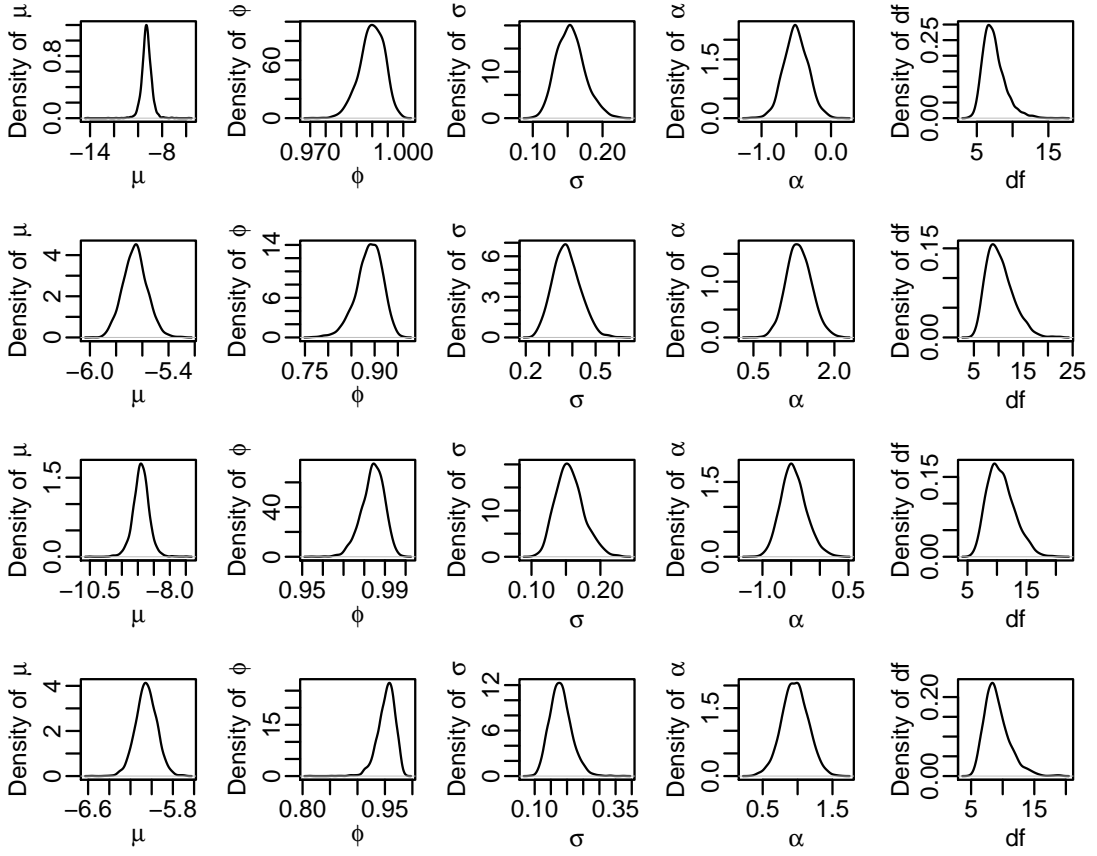


Figure 16: Estimated posterior densities based on 2500 MCMC draws after a burn in of 1000 and thinning with factor 10 for the parameters of the univariate skew Student t stochastic volatility models for SPX, VIX, DAX and VDAX (from top to bottom row).

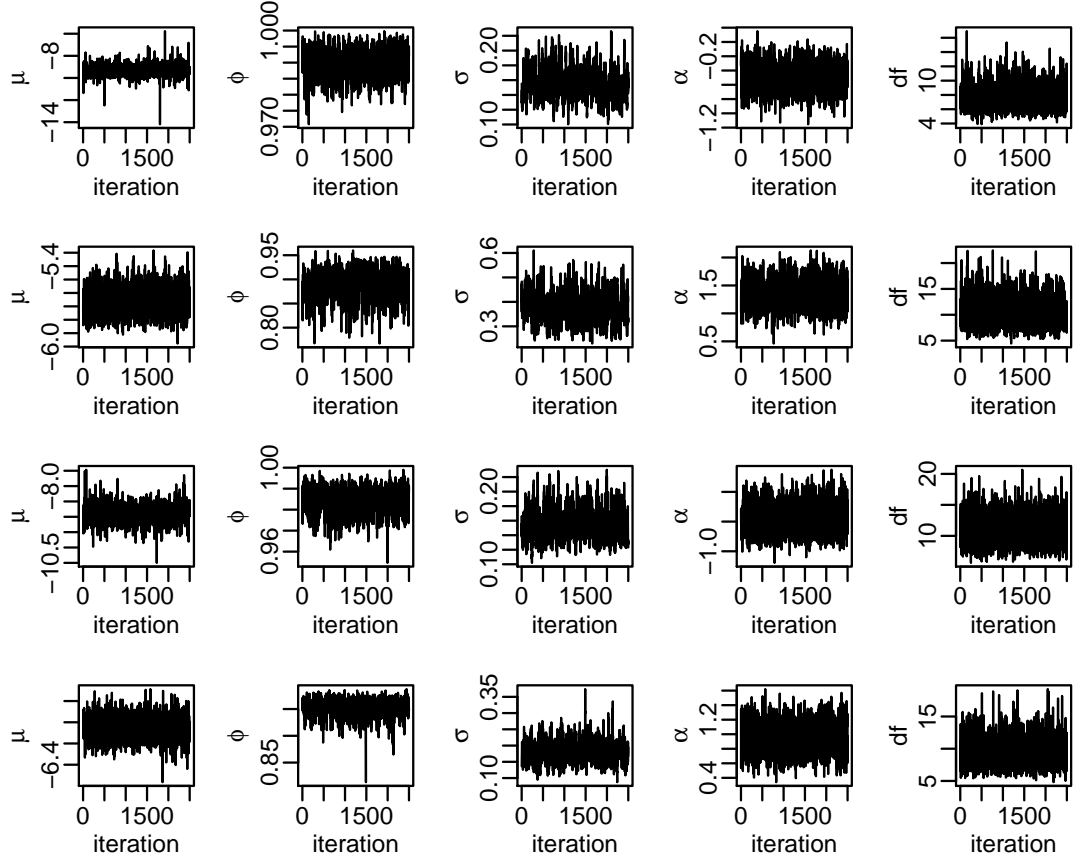


Figure 17: Trace plots of 2500 MCMC draws after a burn in of 1000 and thinning with factor 10 for parameters of the univariate skew Student t stochastic volatility models for SPX, VIX, DAX and VDAX (from top to bottom row).

Results for the dependence models

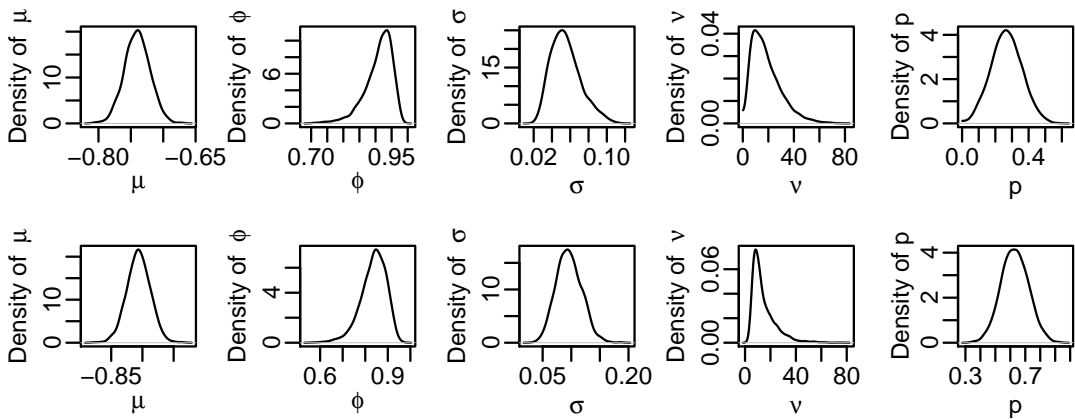


Figure 18: Estimated posterior densities based on 2500 MCMC draws after a burn in of 1000 and thinning with factor 10 for parameters of the dynamic mixture copula model for (SPX,VIX) in the top row and for (DAX,VDAX) in the bottom row.

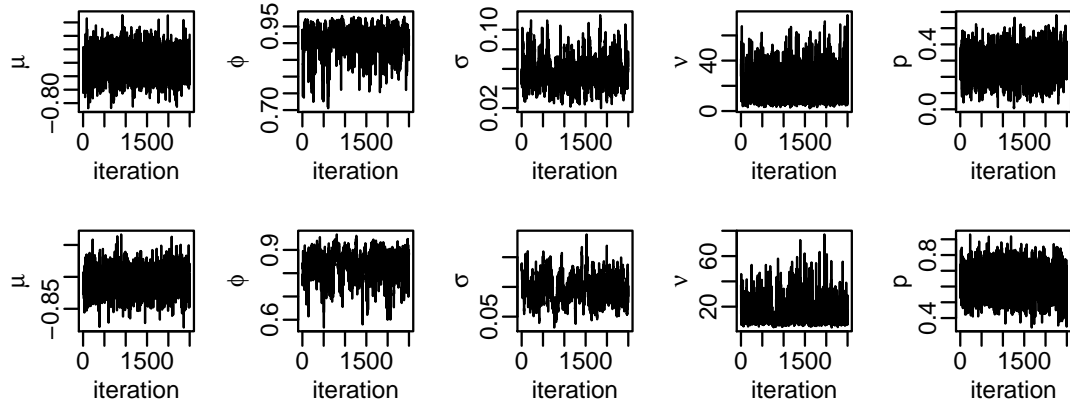


Figure 19: Trace plots of 2500 MCMC draws after a burn in of 1000 and thinning with factor 10 for parameters of the dynamic mixture copula model for (SPX,VIX) in the top row and for (DAX,VDAX) in the bottom row.

References

- Aas K (2016) Pair-copula constructions for financial applications: A review. *Econometrics* 4(4):43
- Aas K, Czado C, Frigessi A, Bakken H (2009) Pair-copula constructions of multiple dependence. *Insurance: Mathematics and economics* 44(2):182–198
- Abanto-Valle C, Lachos V, Dey DK (2015) Bayesian estimation of a skew-student-t stochastic volatility model. *Methodology and Computing in Applied Probability* 17(3):721–738
- Allen DE, Singh AK, Powell RJ, McAleer M, Taylor J, Thomas L (2012) The Volatility-Return Relationship: Insights from Linear and Non-Linear Quantile Regressions
- Almeida C, Czado C (2012) Efficient Bayesian inference for stochastic time-varying copula models. *Computational Statistics & Data Analysis* 56(6):1511–1527
- Azzalini A, Capitanio A (2003) Distributions generated by perturbation of symmetry with emphasis on a multivariate skew t-distribution. *Journal of the Royal Statistical Society: Series B (Statistical Methodology)* 65(2):367–389
- Bates D, Eddelbuettel D, et al (2013) Fast and elegant numerical linear algebra using the RcppEigen package. *Journal of Statistical Software* 52(5):1–24
- Bedford T, Cooke RM (2001) Probability density decomposition for conditionally dependent random variables modeled by vines. *Annals of Mathematics and Artificial intelligence* 32(1-4):245–268
- Bennett J, Grout R, Pébay P, Roe D, Thompson D (2009) Numerically stable, single-pass, parallel statistics algorithms. In: *Cluster Computing and Workshops, 2009. CLUSTER'09. IEEE International Conference on*, IEEE, pp 1–8
- Bitto A, Frühwirth-Schnatter S (2018) Achieving shrinkage in a time-varying parameter model framework. *Journal of Econometrics*
- Bollerslev T (1986) Generalized autoregressive conditional heteroskedasticity. *Journal of econometrics* 31(3):307–327
- Brechmann EC, Czado C (2013) Risk management with high-dimensional vine copulas: An analysis of the Euro Stoxx 50. *Statistics & Risk Modeling* 30(4):307–342
- Brockwell PJ, Davis RA, Calder MV (2002) *Introduction to time series and forecasting*, vol 2. Springer

- Carlin BP, Polson NG, Stoffer DS (1992) A Monte Carlo approach to nonnormal and nonlinear state-space modeling. *Journal of the American Statistical Association* 87(418):493–500
- Chan JC, Grant AL (2016) Modeling energy price dynamics: GARCH versus stochastic volatility. *Energy Economics* 54:182–189
- Eddelbuettel D, François R, Allaire J, Ushey K, Kou Q, Russel N, Chambers J, Bates D (2011) Rcpp: Seamless R and C++ integration. *Journal of Statistical Software* 40(8):1–18
- Engle R (2002) Dynamic conditional correlation: A simple class of multivariate generalized autoregressive conditional heteroskedasticity models. *Journal of Business & Economic Statistics* 20(3):339–350
- Engle RF (1982) Autoregressive conditional heteroscedasticity with estimates of the variance of United Kingdom inflation. *Econometrica: Journal of the Econometric Society* pp 987–1007
- Engle RF, Sheppard K (2001) Theoretical and empirical properties of dynamic conditional correlation multivariate GARCH. Tech. rep., National Bureau of Economic Research
- Fink H, Klimova Y, Czado C, Stöber J (2017) Regime switching vine copula models for global equity and volatility indices. *Econometrics* 5(1):3
- Frühwirth-Schnatter S, Sögner L (2003) Bayesian estimation of the Heston stochastic volatility model. In: *Operations Research Proceedings 2002*, Springer, pp 480–485
- Garthwaite PH, Fan Y, Sisson SA (2016) Adaptive optimal scaling of Metropolis–Hastings algorithms using the Robbins–Monro process. *Communications in Statistics-Theory and Methods* 45(17):5098–5111
- Geman S, Geman D (1984) Stochastic relaxation, Gibbs distributions, and the Bayesian restoration of images. *IEEE Transactions on pattern analysis and machine intelligence* (6):721–741
- Ghalanos A (2012) rmgarch: Multivariate GARCH models. R package version 098
- Gneiting T, Raftery AE (2007) Strictly proper scoring rules, prediction, and estimation. *Journal of the American Statistical Association* 102(477):359–378
- Gruber L, Czado C, et al (2015) Sequential bayesian model selection of regular vine copulas. *Bayesian Analysis* 10(4):937–963
- Hafner CM, Manner H (2012) Dynamic stochastic copula models: Estimation, inference and applications. *Journal of Applied Econometrics* 27(2):269–295
- Hahn PR, He J, Lopes H (2016) Elliptical slice sampling for Bayesian shrinkage regression with applications to causal inference. URL http://faculty.chicagobooth.edu/richard_hahn/research.html
- Joe H (2014) *Dependence modeling with copulas*. CRC Press
- Joe H, Xu JJ (1996) The estimation method of inference functions for margins for multivariate models
- Jondeau E (2016) Asymmetry in tail dependence in equity portfolios. *Computational Statistics & Data Analysis* 100:351–368
- Kastner G (2016a) Dealing with stochastic volatility in time series using the R package stochvol. *Journal of Statistical software* 69(5):1–30
- Kastner G (2016b) Sparse Bayesian time-varying covariance estimation in many dimensions. arXiv preprint arXiv:160808468
- Kastner G, Frühwirth-Schnatter S (2014) Ancillarity-sufficiency interweaving strategy (ASIS) for boosting MCMC estimation of stochastic volatility models. *Computational Statistics & Data Analysis* 76:408–423

- Kastner G, Frühwirth-Schnatter S, Lopes HF (2017) Efficient Bayesian inference for multivariate factor stochastic volatility models. *Journal of Computational and Graphical Statistics* (just-accepted)
- Kim S, Shephard N, Chib S (1998) Stochastic volatility: likelihood inference and comparison with ARCH models. *The review of economic studies* 65(3):361–393
- Loaiza-Maya R, Smith MS, Maneeasoonthorn W (2018) Time series copulas for heteroskedastic data. *Journal of Applied Econometrics* 33(3):332–354
- Min A, Czado C (2011) Bayesian model selection for D-vine pair-copula constructions. *Canadian Journal of Statistics* 39(2):239–258
- Murray I, Adams R, MacKay D (2010) Elliptical slice sampling. In: *Proceedings of the Thirteenth International Conference on Artificial Intelligence and Statistics*, pp 541–548
- Nagler T, Vatter T (2018) rvinecopulib: High performance algorithms for vine copula modeling. R package version 02 5(0)
- Nagler T, Bumann C, Czado C (2018) Model selection in sparse high-dimensional vine copula models with application to portfolio risk. *arXiv preprint arXiv:180109739*
- Nakajima J, Kasuya M, Watanabe T (2011) Bayesian analysis of time-varying parameter vector autoregressive model for the Japanese economy and monetary policy. *Journal of the Japanese and International Economies* 25(3):225–245
- Neal RM (1998) Regression and classification using Gaussian process priors. *Bayesian statistics* 6:475
- Neal RM (2003) Slice sampling. *Annals of statistics* pp 705–741
- Nikoloulopoulos AK, Joe H, Li H (2012) Vine copulas with asymmetric tail dependence and applications to financial return data. *Computational Statistics & Data Analysis* 56(11):3659–3673
- Patton AJ (2006) Modelling asymmetric exchange rate dependence. *International economic review* 47(2):527–556
- Primiceri GE (2005) Time varying structural vector autoregressions and monetary policy. *The Review of Economic Studies* 72(3):821–852
- Robbins H, Monro S (1985) A stochastic approximation method. In: *Herbert Robbins Selected Papers*, Springer, pp 102–109
- Roberts GO, Gelman A, Gilks WR, et al (1997) Weak convergence and optimal scaling of random walk Metropolis algorithms. *The annals of applied probability* 7(1):110–120
- Roberts GO, Rosenthal JS, et al (2001) Optimal scaling for various Metropolis-Hastings algorithms. *Statistical science* 16(4):351–367
- Scheuerer M, Hamill TM (2015) Variogram-based proper scoring rules for probabilistic forecasts of multivariate quantities. *Monthly Weather Review* 143(4):1321–1334
- Schwert GW (1989) Why does stock market volatility change over time? *The journal of finance* 44(5):1115–1153
- Shephard N, Pitt MK (1997) Likelihood analysis of non-Gaussian measurement time series. *Biometrika* 84(3):653–667
- Sklar A (1959) Fonctions de répartition à n dimensions et leurs marges. *Publications de l’Institut de Statistique de l’Université de Paris* 8:229–231
- Smith MS (2015) Copula modelling of dependence in multivariate time series. *International Journal of Forecasting* 31(3):815–833

- Strickland CM, Martin GM, Forbes CS (2008) Parameterisation and efficient MCMC estimation of non-Gaussian state space models. *Computational Statistics & Data Analysis* 52(6):2911–2930
- Vatter T, Chavez-Demoulin V (2015) Generalized additive models for conditional dependence structures. *Journal of Multivariate Analysis* 141:147–167
- Vatter T, Nagler T (2018) Generalized additive models for pair-copula constructions. *Journal of Computational and Graphical Statistics* (just-accepted):1–34
- Watanabe T, Omori Y (2004) A multi-move sampler for estimating non-Gaussian time series models: Comments on Shephard & Pitt (1997). *Biometrika* pp 246–248
- Yu J (2002) Forecasting volatility in the New Zealand stock market. *Applied Financial Economics* 12(3):193–202
- Yu Y, Meng XL (2011) To center or not to center: That is not the question—an Ancillarity–Sufficiency Interweaving Strategy (ASIS) for boosting MCMC efficiency. *Journal of Computational and Graphical Statistics* 20(3):531–570